DOE/ER/13791--T2

TECHNICAL PROGRESS REPORT

1990-1993

Award Number: DE-FG02-87ER13791

Project Title: Photoinitiated Electron Transfer in Multichromophoric Species: Synthetic Tetrads and Pentads

Project Directors: J. Devens Gust, Jr., Thomas A. Moore, Ana L. Moore

Institution: Department of Chemistry and Biochemistry,
Arizona State University
Tempe, AZ 85287-1604

Date: March, 1993

Table of Contents

Technical Progress Report, 1990-1993

A. Research Goals.

This project involves the design, synthesis and study of molecules which mimic some of the important aspects of photosynthetic electron and energy transfer. Solar energy conversion by photosynthesis is the ultimate energy source for essentially all life. In addition, most of mankind's energy needs are met by "fossilized" solar energy in the form of petroleum, coal and natural gas. Because photosynthesis is one of the most durable and, in its early steps, most efficient solar conversion "technologies", an understanding of the details of the process is crucial. This research project is leading to a better understanding of the energy conserving steps of photosynthesis via the study of synthetic model systems which abstract features of the natural photosynthetic apparatus. The knowledge gained from these studies will aid in the design of artificial photosynthetic reaction centers which employ the basic chemistry and physics of photosynthesis to help meet mankind's energy needs.

The approach to artificial photosynthesis employed in this project is to use synthetic pigments, electron donors, and electron acceptors similar to those found in biological reaction centers, but to replace the protein component with covalent bonds. These chemical linkages determine the electronic coupling between the various moieties by controlling separation, relative orientation, and overlap of electronic orbitals. The model systems are designed to mimic the following aspects of natural photosynthetic electron transfer: electron donation from a tetrapyrrole excited singlet state, electron transfer between tetrapyrroles, electron transfer from tetrapyrroles to quinones, and electron transfer between quinones with different redox properties. In addition, they mimic carotenoid antenna function in photosynthesis (singlet-singlet energy transfer from carotenoid polyenes to chlorophyll) and carotenoid photoprotection from singlet oxygen damage (triplet-triplet energy transfer from chlorophyll to carotenoids). An aspect of the natural process which has been of particular interest to this research group is the multistep energy and electron transfer strategy which the natural photosynthetic apparatus uses to great advantage to maximize quantum yields, stored energy, and the lifetimes of charge-separated states.

A major emphasis in research during the last three years has been the design, synthesis and spectroscopic study of molecular pentads which mimic photosynthetic energy and electron transfer. Progress in this area will be the first topic addressed in this report.

B. Synthesis and Photochemistry of C-P-P-Q-Q Pentads.

This part of the project involved the synthesis and study of molecular pentads **1** - **5**, each

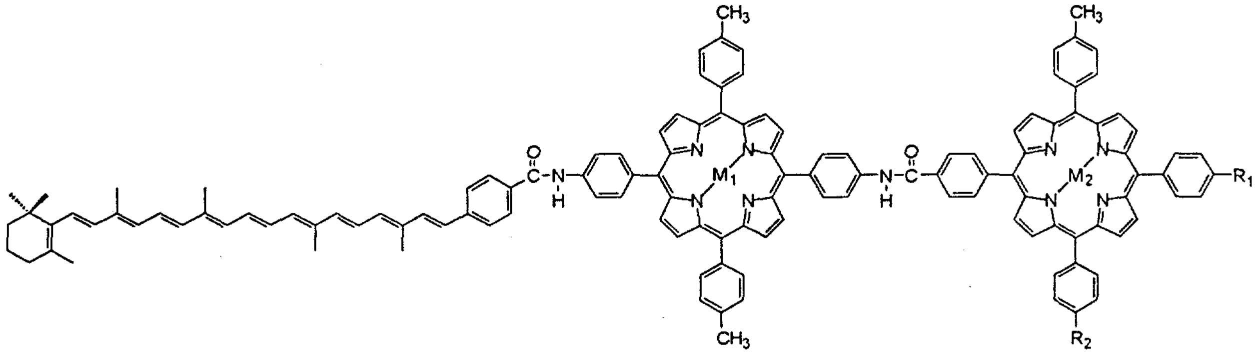

1: $M_1 = H_2$, $M_2 = H_2$, $R_2 = CH_3$, R_1 =

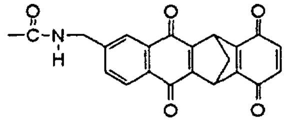

2: $M_1 = Zn$, $M_2 = H_2$, $R_2 = CH_3$, R_1 =

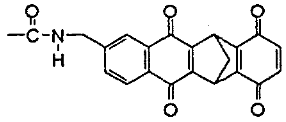

3: $M_1 = Zn$, $M_2 = Zn$, $R_2 = CH_3$, R_1 =

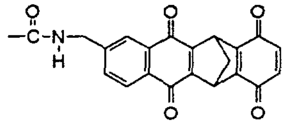

4: $M_1 = Zn$, $M_2 = H_2$, $R_2 = CH_3$, R_1 =

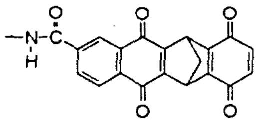

5: $M_1 = Zn$, $M_2 = H_2$, $R_1 = CH_3$, R_2 =

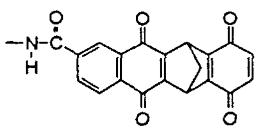

of which consists of a synthetic porphyrin dyad linked to a carotenoid polyene and a diquinone electron acceptor. These molecules all undergo energy and electron transfer processes leading from porphyrin first excited singlet states to long-lived, energetic charge separated states. The study of this series of closely related molecules has enabled us to evaluate the effects of changes in thermodynamic driving force, electronic coupling between the various moieties, and solvent on the rates and therefore the yields of electron transfer steps. The resulting knowledge has been used to design a new pentad molecule which should exhibit interporphyrin photoinduced electron transfer with a quantum yield of charge separation approaching unity. The structure of this new species and its proposed synthesis and study are discussed in the accompanying research proposal. The preparation and photochemical study of this new pentad will provide an excellent test of our ability to carry out molecular engineering of such complex molecules in order to prepare artificial reaction centers with specific properties.

We will begin our summary of the pentad results with a brief description of the photochemistry of two simpler models, **6** and **7**. The details of the synthesis and study of the pentads appear in a manuscript submitted to the *Journal of the American Chemical Society*[1] and a preliminary report in *Science.*[2]

Dyad 6. Porphyrin dyad **6** consists of two very similar tetraarylporphyrin moieties joined by an amide linkage. Both ^1H NMR studies and molecular mechanics calculations show that the partial double bond character of the amide restricts the molecule to extended conformations in which the porphyrins are directed out, away from one another, rather than folded arrangements.

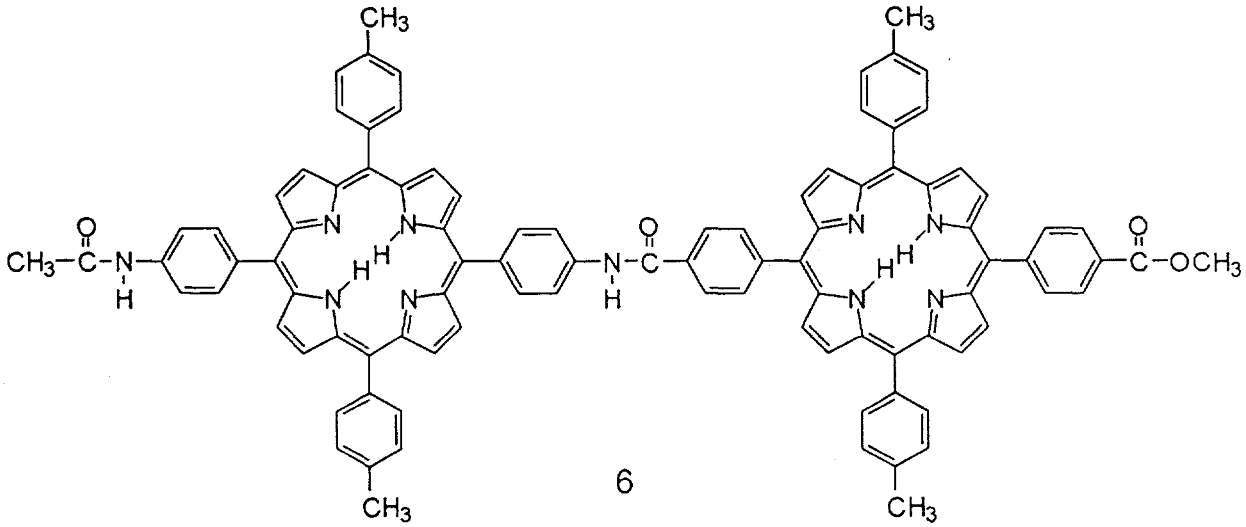

6

Thus, the interporphyrin separation (~19 Å center-to-center) is well-defined, although the interporphyrin dihedral angles are not known with certainty. The absorption spectrum of **6** in dichloromethane features maxima at 422, 518, 554, 594, and 650-nm, and is virtually identical with a linear combination of the spectra of model porphyrin monomers.

The corrected fluorescence emission spectrum of **6** in dichloromethane is similar to those of model tetraarylporphyrins, with maxima at 655 and 720 nm. The lifetime of the excited singlet states following excitation at 590 nm, as measured by observation of the fluorescence decay, is 7.8 ns, which is virtually identical to those of model porphyrin monomers. Thus, linking the chromophores has not introduced any new pathways for quenching of the first excited singlet states. In particular, photoinduced electron transfer to yield a $P^{\bullet+}$-$P^{\bullet-}$ charge-separated state does not occur because photoinduced electron transfer is endergonic, and cannot compete with the usual deactivation pathways.

Tetrad 7. With these results in mind, we turn to P-P-Q_A-Q_B tetrad 7, which consists of a diporphyrin moiety similar to **6** bearing a diquinone electron acceptor species. The diquinone features a naphthoquinone group linked to a benzoquinone via a rigid, bicyclic bridge. This rigidity, coupled with that of the amide linkage, prevents the molecule from folding back on itself and "short-circuiting" the electron transfer processes described below. The absorption spectrum of 7 in dichloromethane in the visible is identical to that of dyad **6**, within experimental error, as is the fluorescence emission spectrum. Global analysis of the porphyrin fluorescence decay

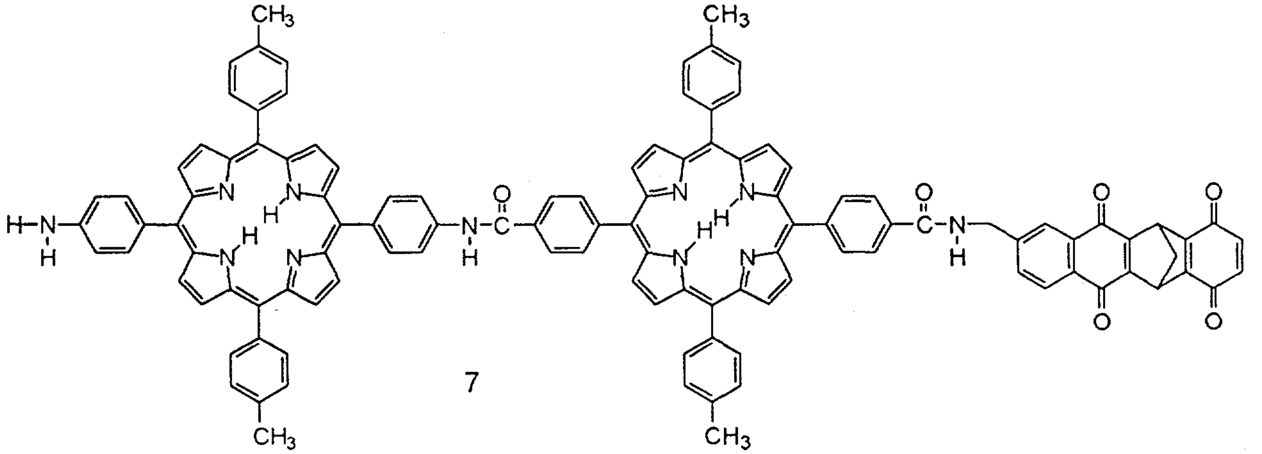

7

following excitation with a 590-nm laser pulse yields a single exponential process with a lifetime of 4.5 ns. The shortened lifetime relative to that for **6** indicates that the porphyrin first excited singlet states are being quenched. The quenching is ascribed to electron transfer from $P\text{-}^1P\text{-}Q_A\text{-}Q_B$ to the naphthoquinone to yield the $P\text{-}P^{\bullet+}\text{-}Q_A{}^{\bullet-}\text{-}Q_B$ charge-separated state, a process which is exergonic by ~0.25 eV. The observation of a single lifetime shows that the two porphyrin moieties exchange excitation energy via singlet-singlet energy transfer which is rapid on the time scale of porphyrin singlet decay. Kinetic analysis of the decay pathways[1] for **7** allows determination of the photoinduced electron transfer rate constant as $1.9 \times 10^8\ s^{-1}$. The quantum yield of electron transfer equals 0.43.

Given the formation of $P\text{-}P^{\bullet+}\text{-}Q_A{}^{\bullet-}\text{-}Q_B$ in **7**, it is clear that from a thermodynamic point of view, the charge-separated state could either recombine to the ground state or undergo additional electron transfer steps to yield new charge-separated species. The latter possibility has been investigated through the synthesis and study of the pentad molecules.

Pentad 1. Pentad **1** was prepared from tetrad **7** by linking a synthetic carotenoid to the amino group.[1] Molecular mechanics and NMR data show that the conformation of the molecule is extended, with an overall length of ~80 Å. The absorption spectrum in dichloromethane features porphyrin Q-bands at 650, 594, ~554 and ~518 nm, a Soret band at 422 nm, and quinone absorptions at < 400 nm. Superimposed upon these bands is the carotenoid absorption, with maxima in the 450 - 520 nm region. The shape of the fluorescence emission spectrum of **1** is identical to those of **6** and **7**, with maxima at 655 and 720 nm.

Fluorescence decay measurements of **1** in dichloromethane were carried out with laser excitation at 590 nm. A satisfactory fit to all the data was obtained using two exponential components with lifetimes of 3.09 and 1.85 ns. The minor component with the shorter lifetime likely represents an impurity. The results of this experiment may be interpreted by reference to Scheme I, which shows the relevant transient states. Excitation yields an essentially equimolar mixture of $C\text{-}P\text{-}^1P\text{-}Q_A\text{-}Q_B$ and $C\text{-}^1P\text{-}P\text{-}Q_A\text{-}Q_B$. These two species undergo rapid singlet-singlet energy transfer and decay via various photochemical processes (steps 3 and 4) and electron transfer by step 2 to yield C-P-P$^{\bullet+}$-Q$_A^{\bullet-}$-Q$_B$. The rate constants for steps 3 and 4 may be estimated as 2.9×10^8 s^{-1} and 1.2×10^8 s^{-1} based on results for model compounds. These data may be used to calculate a value for k_2 of 2.3×10^8 s^{-1}, which is very similar to the corresponding rate constant determined above for 7. The quantum yield Φ_2 for the C-P-P$^{\bullet+}$-Q$_A^{\bullet-}$-Q$_B$ charge-separated state is 0.36. Thus, appending the carotenoid to tetrad 7 has essentially no effect upon the rate constant for photoinduced electron transfer.

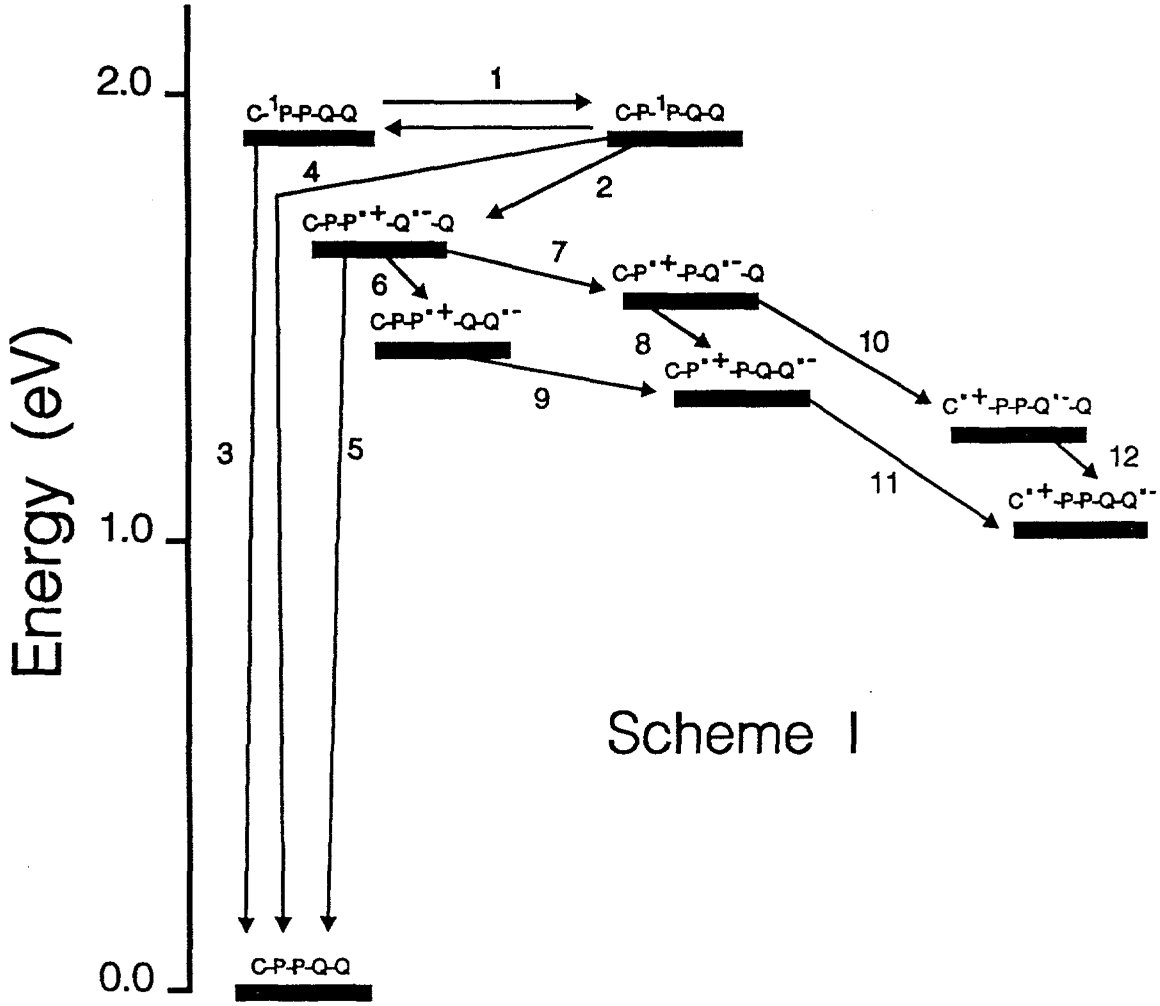

Scheme I

Scheme I suggests that although C-P-P$^{\bullet+}$-Q$_A^{\bullet-}$-Q$_B$ undoubtedly decays rapidly by step 5, electron transfer via steps 6 and 7 could compete with charge recombination, beginning an electron transfer cascade that would converge on a final C$^{\bullet+}$-P-P-Q$_A$-Q$_B^{\bullet-}$ species. Transient absorption spectroscopy on the ns time scale was used to investigate this possibility. Excitation of a dichloromethane solution of **1** with a 10-ns laser pulse at 590 nm resulted in the observation of a strong transient absorption with a maximum at ~960 nm. This absorption can be assigned to the carotenoid radical cation, and ascribed to the $C^{\bullet+}$-P-P-Q_A-$Q_B^{\bullet-}$ charge-separated state. Thus, electron transfer occurs via at least some of the pathways 6 - 12 in Scheme I. The overall quantum yield of $C^{\bullet+}$-P-P-Q_A-$Q_B^{\bullet-}$ was estimated as 0.15 using the comparative method. The lifetime of $C^{\bullet+}$-P-P-Q_A-$Q_B^{\bullet-}$ was ~340 μs.

Pentad 2. The quantum yield data for pentad **1** show that a major loss of quantum efficiency results from inefficient competition of the secondary or "dark" electron transfer reactions with charge recombination of the various charge-separated states shown in Scheme I. Step 5 is likely to be the major contributor to this recombination, as the positive and negative charges are in closest proximity in this species. Thus, the overall efficiency of charge separation might be enhanced by increasing the rate of step 6 and/or 7. Zinc-containing pentad **2** was designed to investigate this strategy. Insertion of the zinc ion results in stabilization of the porphyrin radical cation by 0.21 eV, and therefore a comparable increase in the thermodynamic driving force for step 7. The energies of the various transient states of **2** are shown in Scheme II.

Fluorescence studies were carried out in both dichloromethane and chloroform solutions. In both solvents, the emission spectra were similar to those observed for the free base porphyrins of **6**, **7**, and **1**, with maxima at 655 and 720 nm. Excitation at wavelengths where absorption was due mainly to the zinc porphyrin resulted in an additional very weak emission band at 611 nm which is ascribed to the zinc porphyrin. The emission from the free base porphyrin is quenched relative to that from a model porphyrin, as was the case for **7** and **1**. The emission from the zinc porphyrin was quenched much more strongly, which is consistent with rapid singlet-singlet energy transfer from the zinc porphyrin to the free base. Indeed, steady-state fluorescence excitation studies showed that singlet-singlet transfer is nearly complete.

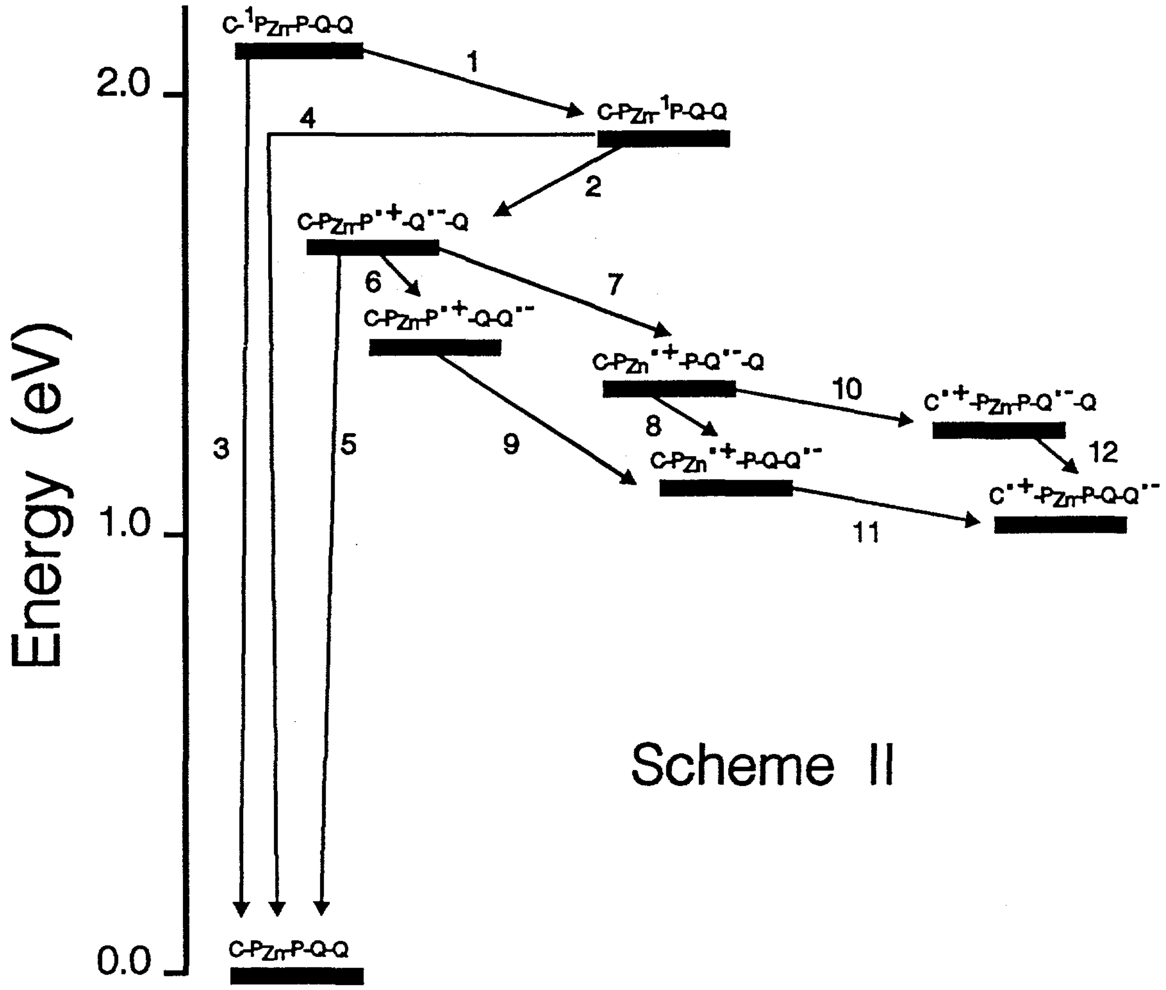

Scheme II

Time resolved fluorescence emission data were obtained for **2** in both chloroform and dichloromethane with excitation at 590 nm. In chloroform, the two significant components had lifetimes of 0.039 and 1.2 ns (Figure 1). Excitation at 650 nm, where only the free base porphyrin absorbs, yielded spectra featuring the 1.2 ns decay, but lacking the 39-ps component.

The 39-ps component may be associated with the decay of $C\text{-}{}^1P_{Zn}\text{-}P\text{-}Q_A\text{-}Q_B$, mainly by singlet-singlet energy transfer to the free base porphyrin. The rate constant for singlet-singlet transfer (k_1 in the Scheme) equals 2.3×10^{10} s^{-1}, and the quantum yield is 0.90, which is consistent with the fluorescence excitation results discussed above.

The other significant component of the fluorescence decay of pentad **2** is due to the free base porphyrin moiety. The short lifetime relative to that of a model porphyrin (7.8 ns in

Figure 1

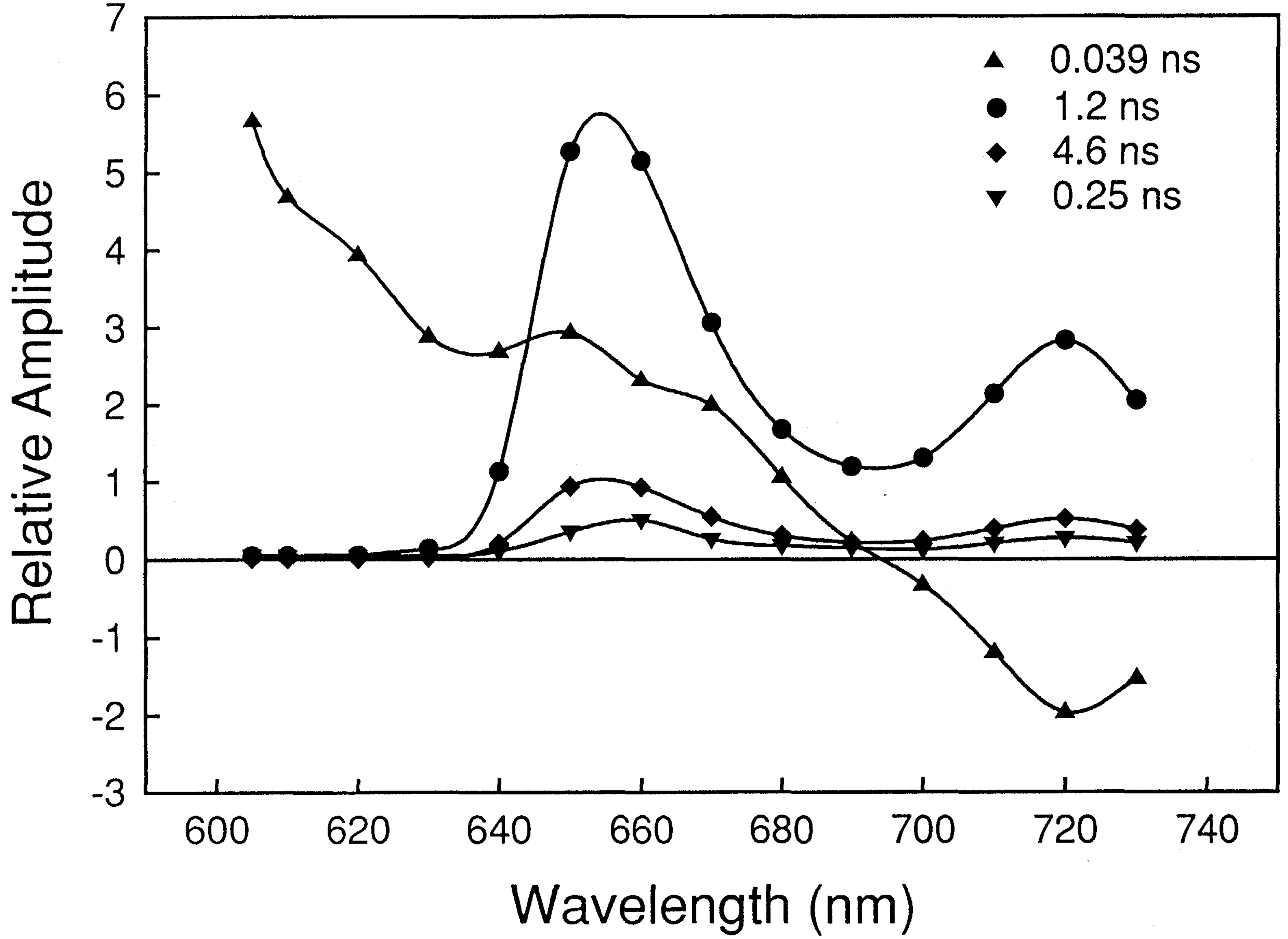

Relative Amplitude
7
6
5
4
3
2
1
0
-1
-2
-3
600
620
640
660
680
700
720
740
Wavelength (nm)
▲ 0.039 ns
● 1.2 ns
◆ 4.6 ns
▼ 0.25 ns

chloroform) is consistent with the quenching of the steady-state fluorescence intensity. The decreased lifetime is attributed to electron transfer via step 2 in Scheme II, which is similar to that observed in **1** and **7**. The rate constant for this photoinitiated electron transfer equals 7.1×10^8 s^{-1}. The corresponding quantum yield, based on C-P_{Zn}-^{1}P-Q_A-Q_B, is $k_2 \times \tau_f$, or 0.85.

Similar decay associated spectra were obtained for **2** in dichloromethane solution. The lifetime of C-$^1P_{Zn}$-P-Q_A-Q_B was found to be 0.035 ns, whereas that of C-P_{Zn}-^{1}P-Q_A-Q_B was 2.46 ns. The data yield a value of 2.5×10^{10} s^{-1} for k_1, which is virtually identical to that measured in chloroform, and a quantum yield for singlet-singlet transfer of 0.89. The photoinduced electron transfer rate constant (k_2) is 2.9×10^8 s^{-1}, and the corresponding quantum yield is 0.71.

Scheme II shows that C-P_{Zn}-$P^{\bullet +}$-$Q_A^{\bullet -}$-Q_B can in principle recombine via step 5 or evolve through steps 6, 7 and subsequent electron transfers to yield $C^{\bullet +}$-P_{Zn}-P-Q_A-$Q_B^{\bullet -}$. Excitation of **2** in chloroform solution with a 650-nm laser pulse led to the formation of a long-lived transient absorption with a maximum at 970 nm which was assigned to the carotenoid radical cation of the $C^{\bullet +}$-P_{Zn}-P-Q_A-$Q_B^{\bullet -}$ charge-separated state. The lifetime of this state was 55 μs, and its overall quantum yield was 0.83. Formation of a long-lived charge-separated state was also observed in dichloromethane. The lifetime of $C^{\bullet +}$-P_{Zn}-P-Q_A-$Q_B^{\bullet -}$, ~200 μs, was longer than that in chloroform, but the quantum yield was reduced to 0.60.

Pentad 3. The form of the pentad in which both porphyrin moieties are metallated was easily prepared by stirring a solution of **1** with an excess of zinc acetate. The absorption spectrum of **3** in dichloromethane features carotenoid and quinone bands similar to those observed for **1** and **2** and typical zinc porphyrin absorptions at 590, 548 and 424 nm. The emission spectrum is also typical of a zinc porphyrin, with maxima at 602 and 650 nm. Time resolved fluorescence emission studies were performed as described above in dichloromethane solution with excitation at 590 nm. Global analysis yielded a lifetime of 0.23 ns. The results are consistent with rapid singlet-singlet energy transfer between the two porphyrin first excited singlet states, which are essentially isoenergetic at 2.07 eV, and decay of these two species by the usual routes (steps 3 and 4 in

Scheme III) and by electron transfer to the attached naphthoquinone via step 2. The electron transfer rate constant k_2 is 4.8×10^9 s^{-1} and the quantum yield of $C\text{-}P_{Zn}\text{-}P_{Zn}^{\bullet+}\text{-}Q_A^{\bullet-}\text{-}Q_B$, is 0.55.

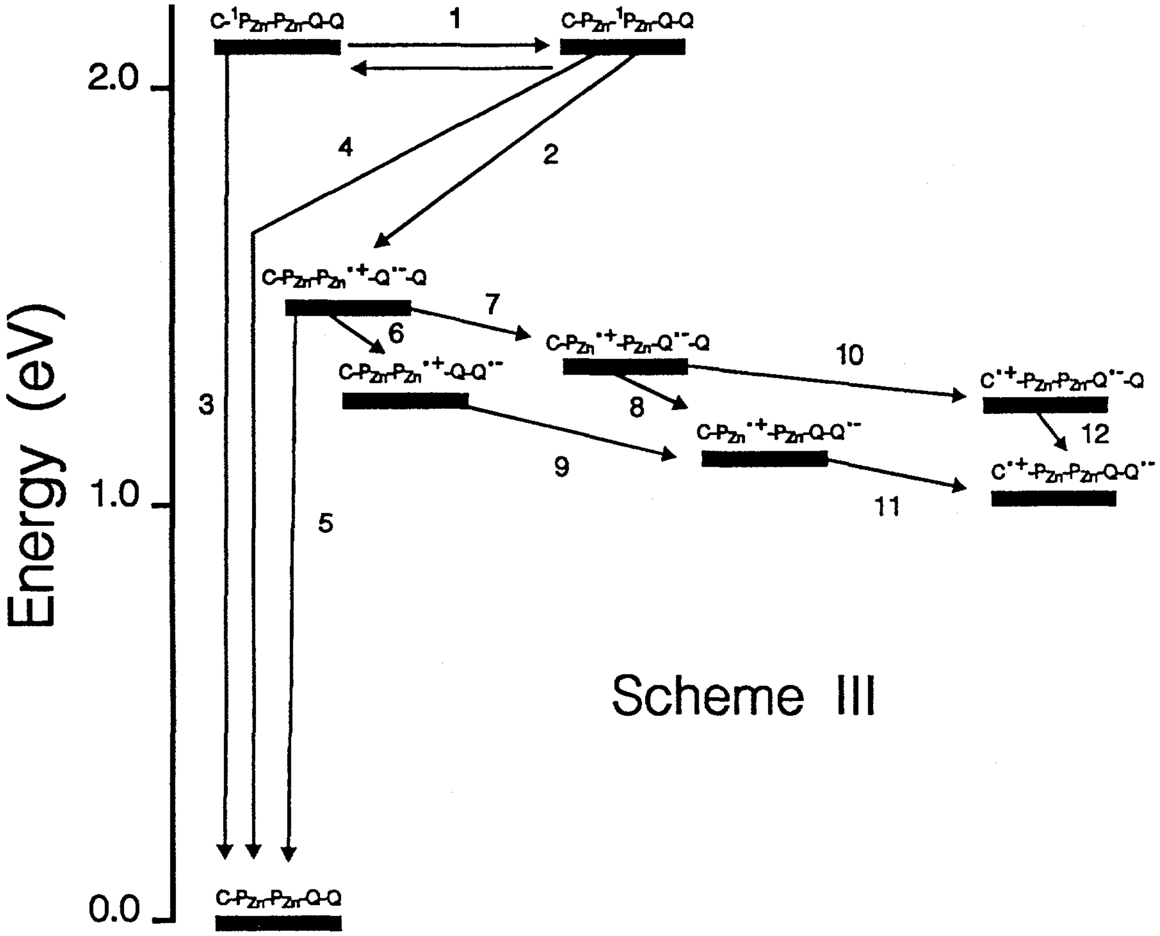

Scheme III

Transient absorption studies of **3** in dichloromethane with 590-nm laser excitation showed that as with the pentads discussed above, a long-lived charge separated state, assigned to $C^{\bullet+}\text{-}P_{Zn}\text{-}P_{Zn}\text{-}Q_A\text{-}Q_B^{\bullet-}$, was formed. The quantum yield was 0.15, and the lifetime was 120 μs.

Pentads With Increased Porphyrin-Quinone Electronic Coupling. The results for pentads **1** - **3** show that in all of these cases, the quantum yield is limited at least in part by the rate of photoinduced electron transfer step 2, which cannot compete with steps 3 and 4 to the extent necessary to achieve a quantum yield of unity. The photoinduced electron transfer step can be made much more rapid, and therefore more efficient, by increasing the electronic coupling between the porphyrin and naphthoquinone. Pentads **4** and **5** were prepared in order to investigate the effects of increased coupling. The structures of these are similar to that of **2**, with the exception that the porphyrin-diquinone linkage is reversed, and the methylene spacer removed. The first reduction potentials of the naphtho- and benzoquinone moieties of the diquinone portions of **4** and **5** are identical within experimental error to those found for pentads **1** and **2**. The first oxidation potential of a model for the free base porphyrin moiety of **4** and **5** is lower by 0.07 eV than that for a comparable model for pentads **1** and **2**. These relatively small differences suggest that any differences in electron transfer rates may be ascribed mainly to the alteration in electronic coupling between the porphyrin and quinone moieties.

Pentad 4. *The steady-state emission spectrum of* **4** *is essentially identical to that of* pentad **2**. Fluorescence decay studies in chloroform were carried out with excitation at 650 nm, where only the free base porphyrin absorbs light. Global analysis yielded a major component with the emission spectrum of the free base porphyrin having a lifetime of 0.014 ns. Thus, the free base porphyrin first excited singlet state is strongly quenched due to electron transfer to the diquinone (step 2 in Scheme IV). Analysis of the fluorescence data yields a value for k_2 of 7.1×10^{10} s^{-1} and a quantum yield of C-P$_{Zn}$-P$^{\bullet+}$-Q$_A$$^{\bullet-}$-Q$_B$ equal to 0.99.

Fluorescence decay studies were also carried out in chloroform with 590-nm excitation. In this case, the free base and metallated porphyrin moieties are both excited, and a mixture of C-P$_{Zn}$-^{1}P-Q$_A$-Q$_B$ and C-^{1}P$_{Zn}$-P-Q$_A$-Q$_B$ is produced. Decays were measured at 8 wavelengths in the 625 - 730-nm region and analyzed globally. The results for **4** and related model systems allow estimation of the rate constants k_1, k_2, k_3 and k_4 in Scheme IV as 2.3×10^{10}, 7.1×10^{10}, 2.7×10^9 and 1.4×10^8 s^{-1}, respectively.

Excitation of a solution of **4** in chloroform with a 10-ns laser pulse at 650 nm resulted in the observation of a carotenoid radical cation spectrum similar to those seen with **1** and **2**. This spectrum is ascribed to the C$^{\bullet+}$-P$_{Zn}$-P-Q$_A$-Q$_B$$^{\bullet-}$ charge-separated state. The quantum yield was 0.28, and the lifetime of the state was 6.8 μs. With 590-nm excitation, the quantum yield dropped to 0.22.

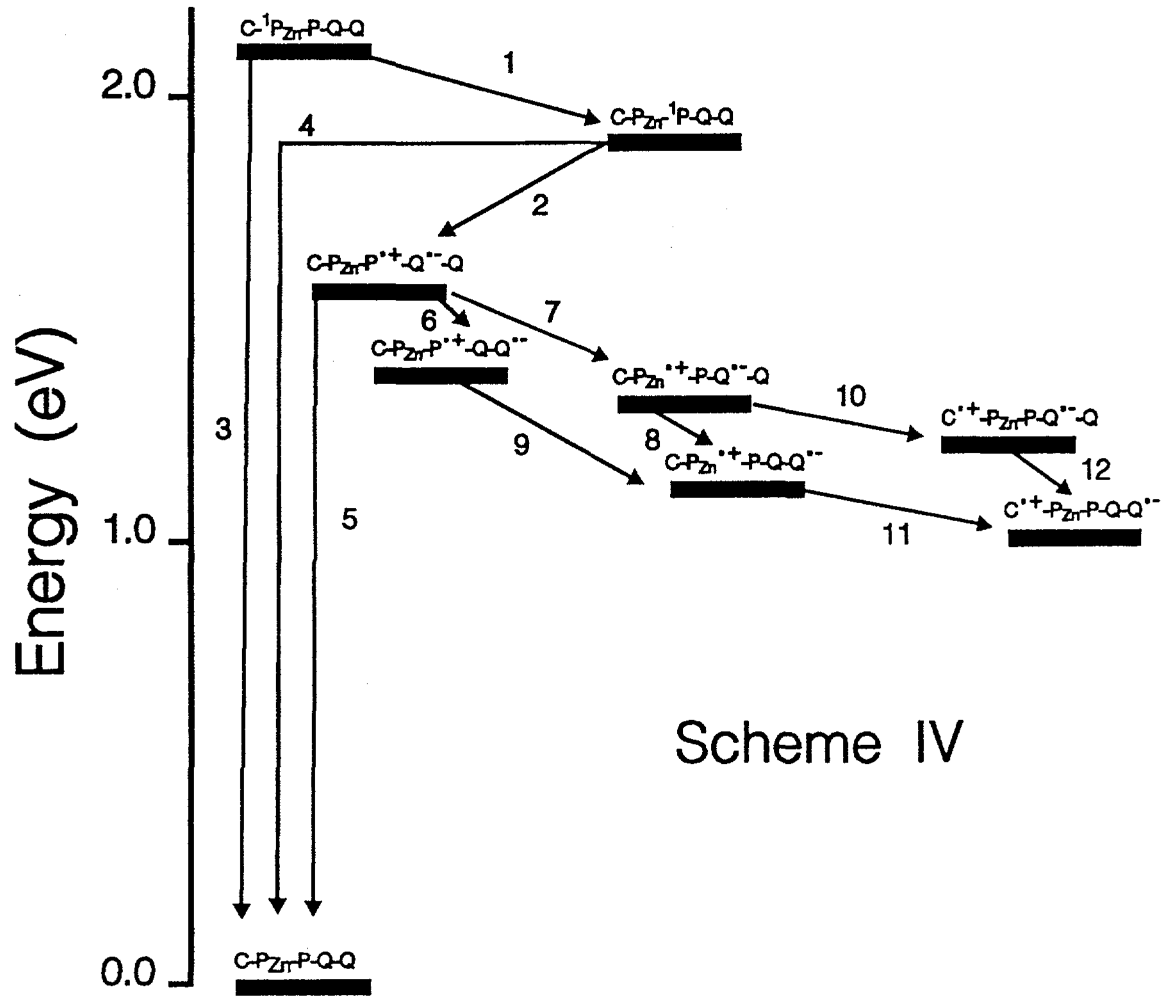

Scheme IV

In dichloromethane solution with 590-nm excitation, pentad **4** yields time resolved fluorescence decay results virtually identical to those obtained in chloroform. Thus, within experimental error, the rate constants estimated above for chloroform solution also apply in dichloromethane. A final $C^{\bullet+}\text{-}P_{Zn}\text{-}P\text{-}Q_A\text{-}Q_B^{\bullet-}$ charge-separated state was again observed by transient absorption spectroscopy. The quantum yield was ~0.04 with either 650-nm or 590-nm excitation, and the lifetime of the final state was 35 µs.

Pentad 5. This pentad is identical in structure to **4**, with the exception that the quinone experiences a 5,10-relationship with the metallated porphyrin, rather than the 5,15-relationship found in **1** - **4**. To a first approximation, this molecule would be expected to have rate constants for photoinduced energy and electron transfer processes which are virtually identical to those found for **4**, if, as suggested by Scheme IV, all of the significant transfers occur between directly linked moieties. Indeed, this is the case for the steps leading to formation of the final $C^{\bullet +}$-P_{Zn}-P-Q_A-$Q_B^{\bullet -}$ state. The results of many multiwavelength fluorescence decay experiments showed that the results for **5** were indistinguishable from those for **4**, within experimental error. Thus values for k_1, k_2, k_3 and k_4 of 2.3×10^{10}, 7.1×10^{10}, 2.7×10^{9} and 1.4×10^{8} s^{-1} are estimated for **5** in both chloroform and dichloromethane.

The formation of a final charge-separated state $C^{\bullet +}$-P_{Zn}-P-Q_A-$Q_B^{\bullet -}$ in 5 was studied using transient absorption spectroscopy. In chloroform solution, excitation of 5 with a laser pulse at either 650 or 590 nm led to the formation of $C^{\bullet +}$-P_{Zn}-P-Q_A-$Q_B^{\bullet -}$ with a quantum yield of 0.25 and a lifetime of only 0.54 μs. Similar experiments in dichloromethane gave a quantum yield of 0.05 and a lifetime of ~34 μs. Thus, pentad **5** behaves in a manner essentially identical to isomer **4**, with the exception of the shorter lifetime for the final charge-separated state in chloroform solution.

Discussion. Within the series of pentads, **2** in chloroform solution gave the highest quantum yield for the final $C^{\bullet +}$-P_{Zn}-P-Q_A-$Q_B^{\bullet -}$ state. Thus, a fruitful way to discuss the results of this study is to compare the results for the other pentads and solvents to those for **2**, and to deduce reasons for any differences.

Pentad 2 in Dichloromethane - Effect of Solvent. When the solvent is changed from chloroform to dichloromethane, the quantum yield of $C^{\bullet +}$-P_{Zn}-P-Q_A-$Q_B^{\bullet -}$ drops from 0.83 to 0.60. There are two reasons for this change. In the first place, the rate constant for photoinduced electron transfer step 2 (Scheme II) in dichloromethane is only about 0.4 times that in chloroform, and this reduces the quantum yield of the initial step from 0.85 to 0.71. Secondly, the change in solvent evidently affects the rates of dark reactions so that steps 6 to 12 in Scheme III are not able to compete as efficiently with charge recombination of the various intermediates.

Pentads 1 and 3 - Effect of Metallation. Although removal of the zinc from pentad 2 does not significantly affect the rate of photoinduced electron transfer step 2, it does result in a substantially lower quantum yield of the initial charge-separated state, C-P-$P^{\bullet+}$-$Q_A^{\bullet-}$-Q_B, in **1** (0.36). This is due in part to the fact that removal of the zinc renders C-^{1}P-P-Q_A-Q_B and C-P-^{1}P-Q_A-Q_B essentially isoenergetic, and this in turn results in rapid singlet-singlet energy transfer between the two porphyrin moieties. Although the decay pathways for C-P-^{1}P-Q_A-Q_B are not directly affected by the carotenoid, the lifetime of C-^{1}P-P-Q_A-Q_B is somewhat reduced by the attached carotene. This quenching is most likely electron or energy transfer between the porphyrin and carotenoid moieties.[3] Thus, when the two porphyrin first excited singlet states are rapidly exchanging singlet excitation, the quantum yield of C-P-$P^{\bullet+}$-$Q_A^{\bullet-}$-Q_B is reduced relative to that in **2** because of the increased rate of decay of C-P-^{1}P-Q_A-Q_B via energy transfer to the porphyrin bearing the carotenoid followed by decay according to step 3. The yield of the final $C^{\bullet+}$-P-P-Q_A-$Q_B^{\bullet-}$ state in **1** is further reduced from 0.36 to 0.15 in dichloromethane due to inefficient competition of steps 6 - 12 in Scheme II with charge recombination. As a first approximation, it is reasonable to postulate that step 5 is the most rapid charge recombination reaction. Although the thermodynamic driving forces for steps 5 and 6 in Scheme I are expected to be essentially identical to those for the comparable steps in pentad **2** (Scheme II), the driving force for step 7 in free-base pentad **1** (0.11 eV) is substantially reduced from that for step 7 in zinc pentad **2** (0.32 eV). As these reaction exergonicities are undoubtedly in the normal region of Marcus theory for electron transfer, step 7 is expected to be substantially slower in **1** than in **2**. This undoubtedly accounts for the decrease in efficiency of the dark reactions.

The dimetallated pentad **3** also has a reduced quantum yield for the final $C^{\bullet+}$-P_{Zn}-P_{Zn}-Q_A-$Q_B^{\bullet-}$species (0.15) relative to **2** (0.60) in dichloromethane. Again, two factors conspire to produce this result. The rate of photoinduced electron transfer for **3**, where the metalloporphyrin is the donor species, is about 17 times greater than that for **2**, where the free-base porphyrin is the donor. At first glance, this enhancement might be expected to result in a higher quantum yield for the initial electron transfer state C-P_{Zn}-$P_{Zn}^{\bullet+}$-$Q_A^{\bullet-}$-Q_B. This is not realized because the zinc porphyrin first excited singlet state C-P_{Zn}-$^1P_{Zn}$-Q_A-Q_B has a substantially shorter lifetime in the absence of electron transfer than does C-P_{Zn}-^{1}P-Q_A-Q_B and because this state rapidly exchanges singlet excitation with $C-{}^1P_{Zn}-P_{Zn}-Q_A-Q_B$, which is also short-lived. Thus, the quantum yield of $C-P_{Zn}-P_{Zn}{}^{\bullet+}-Q_A{}^{\bullet-}-Q_B$ in **3** is only 0.55 in dichloromethane, whereas that of $C-P_{Zn}-P^{\bullet+}-Q_A{}^{\bullet-}-Q_B$ in **2** is 0.71. The yield of $C^{\bullet+}-P_{Zn}-P_{Zn}-Q_A-Q_B{}^{\bullet-}$ in **3** is further reduced by inefficient competition of steps 6 - 12 with charge recombination. This is likely due, for the most part, to the large decrease in driving force, and therefore presumably rate, for step 7 in **3** relative to **2** which results from metallation of both porphyrin moieties (cf. Schemes II and III).

Pentads 4 and 5 - Effect of Electronic Coupling. These two molecules are closely related, and the rate constants for energy transfer and charge separation are identical, within the limits of error of this study. The yields of the final $C^{\bullet+}-P_{Zn}-P-Q_A-Q_B{}^{\bullet-}$ states for these molecules are ~0.25 in chloroform and ~0.05 in dichloromethane. The reduction in quantum yield relative to **2** is not due to the photoinduced electron transfer step 2 (Scheme IV) because this very rapid step occurs with a yield of essentially unity. Therefore, the reduction must be due to inefficient competition with charge recombination. The rate constants for steps 6 and 7 are expected to be essentially identical for **2, 4** and **5**, as these steps do not involve porphyrin-quinone electron transfer and the changes in the porphyrin-quinone linkage have only a small effect on the thermodynamic driving force for these reactions. However, the electronic coupling between the porphyrin and diquinone moieties has been greatly increased in pentads **4** and **5**, relative to **1** - **3**, and this increase evidently increases the rate of charge recombination by step 5, as well as that for step 2. The net result is that competition of steps 6 and 7 with charge recombination is not very efficient, especially in dichloromethane solution.

Lifetimes of the Final Charge-Separated States. In all five pentads, the energies of the final states are expected to be essentially identical under any given set of conditions. Also, pentads **1** - **3** have identical linkages between the various moieties, and therefore molecular conformations and internuclear distances are not expected to differ strongly within this set of molecules. However, the lifetime of the final charge-separated state in dichloromethane varies significantly among the three compounds. In particular, successive introduction of zinc ions into the porphyrin moieties leads to shortening of the lifetimes. This suggests that charge recombination may involve the porphyrin moieties. They could take part through superexchange (through-bond) coupling of the carotenoid radical cation and the benzoquinone radical anion, or via endergonic population of some of the intermediate charge-separated states in the schemes followed by charge recombination. For example, the enhanced stabilization of a positive charge on the porphyrin macrocycle resulting from metallation would facilitate migration of the "hole" from the carotenoid toward the diquinone moiety.

The lifetime of the final state of pentad **4** is substantially shorter than that for the corresponding state of **2** under comparable conditions. This result is consistent with the change in porphyrin-quinone linkage which both brings the carotenoid and benzoquinone moieties spatially closer together and increases the electronic coupling between the porphyrin and diquinone species.

Although the $C^{\bullet+}$-P_{Zn}-P-Q_A-$Q_B^{\bullet-}$ states of **4** and **5** have comparable lifetimes in dichloromethane, the lifetime in chloroform for **5**, which features the 5,10 linkage of the metallated porphyrin and diquinone moieties to the free-base porphyrin, is more than 10 times shorter than that for **4**, with the 5,15 linkage. This shortening likely results from the ability of **5** to assume conformations in chloroform in which the benzoquinone and metallated porphyrin approach one another to a separation of only a few Å. Molecular mechanics calculations of the type discussed earlier show that this is possible even if one considers only changes in dihedral angle resulting from rotations about single bonds. Such conformations may be sampled more frequently in chloroform than dichloromethane. These conformations are precluded in the molecules featuring the 5,15 linkage.

Conclusions. These results allow one to draw several conclusions concerning the construction of artificial photosynthetic reaction centers. In the first place, excitation of pentad **2** in chloroform solution leads to the formation of a $C^{\bullet+}$-P_{Zn}-P-Q_A-$Q_B^{\bullet-}$ charge-separated state with a quantum yield approaching unity which has a long lifetime and preserves about one-half of the original excitation energy as chemical potential. These studies are qualitatively similar to those found for natural bacterial reaction centers. Thus, although a great deal remains to be learned about various aspects of the natural process, these results show that it is possible to mimic its general features in artificial systems which lack a protein component.

Secondly, it will be noted that pentads such as **2** achieve a high level of discrimination against charge recombination reactions by employing two multistep electron transfer strategies. The first is sequential multistep electron transfer such as is observed in natural reaction centers. For example, the photoinduced electron transfer step 2 in pentad **2** yields $\text{C-P}_{\text{Zn}}\text{-P}^{\bullet+}\text{-Q}_{\text{A}}{}^{\bullet-}\text{-Q}_{\text{B}}$, which decays by sequential electron transfer steps whose function is to move the positive charge to the carotenoid end of the molecule and the negative charge to the benzoquinone (e.g. steps 7, 10 and 12). The result is a charge-separated state which is long lived, because of the large spatial separation of the charges, but which is formed in high quantum yield because each step in the sequence is fast relative to charge recombination and therefore efficient. In addition, the pentad uses a parallel multistep electron transfer strategy to advantage. For example, charge recombination step 5 in Scheme II is undoubtedly one of the most rapid charge recombinations because of the proximity of the charges in $\text{C-P}_{\text{Zn}}\text{-P}^{\bullet+}\text{-Q}_{\text{A}}{}^{\bullet-}\text{-Q}_{\text{B}}$. The pentad employs two electron transfer steps, 6 and 7, operating in parallel to compete with this charge recombination. Using this strategy, a higher quantum yield of the final $\text{C}^{\bullet+}\text{-P}_{\text{Zn}}\text{-P-Q}_{\text{A}}\text{-Q}_{\text{B}}{}^{\bullet-}$ state can be achieved than would be possible for one step acting alone with an efficiency of less than unity. This strategy appears not to be used in bacterial reaction centers, but could operate in a reaction center approaching true C_2 symmetry. Both of these strategies are amenable to application in many other sorts of electron and energy transfer systems and chemical reactions in general.

Finally, these results illustrate that although manipulation of individual electron and energy transfer rate constants in the pentads or other complex organic systems based on qualitative application of existing energy and electron transfer theories is relatively facile, structural or environmental changes which affect some rate constants invariably affect others. Thus, rational engineering of structures such as the pentads to increase quantum yields, lifetimes, stored energy, etc., requires a very detailed knowledge of all the effects of a given structural alteration. For example, it is clear that achieving a higher quantum yield of long-lived charge separation in the pentad systems requires a higher yield for photoinduced electron transfer step 1 than was observed in **2**, and therefore a larger rate constant for this step. However, if the electronic coupling between the porphyrin and quinone moieties is increased too much, as occurs with **4** and **5**, an unacceptable increase in the rate of charge recombination by step 5 will result, and the overall quantum yield of the final state will decrease, relative to **2**.

C. Synthesis and Photochemistry of a New C-P-Q-Q Tetrad.

The results for the pentads led us to design a new porphyrin-quinone linkage which we expected to provide more optimal electronic coupling for systems of this type. We have included it in a new tetrad molecule, **8,** in order to evaluate its performance relative to the linkage in previously-reported tetrad **9**,[5,6] which is similar to that in pentads **4** and **5**. This work, which is summarized below, has been submitted for publication in *Chemical Physics*.[5]

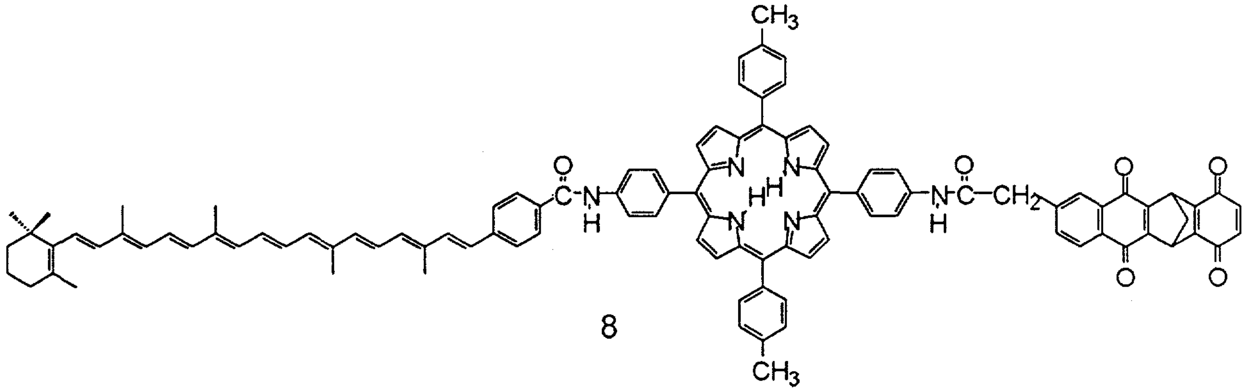
8

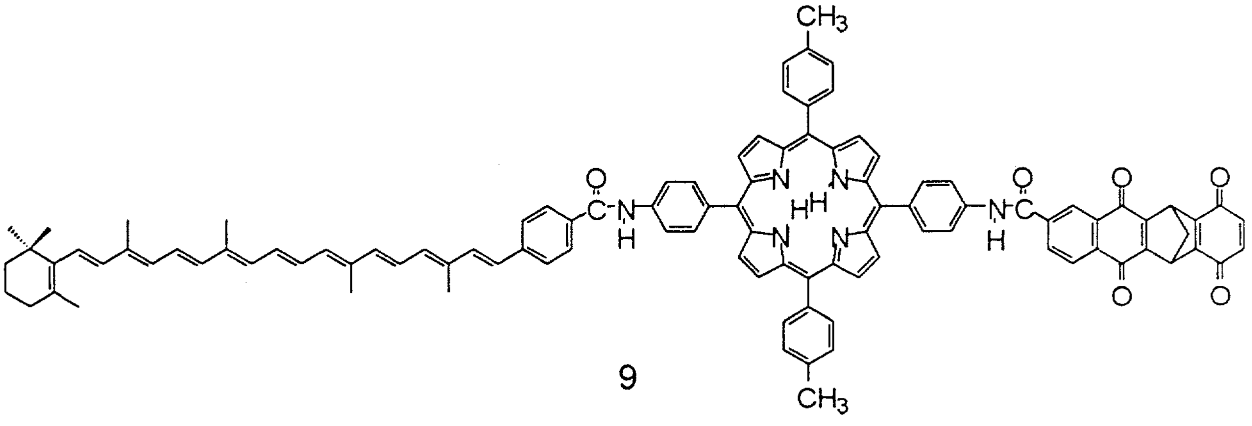
9

Synthesis and Conformation. The synthetic route to **8** is related in its general features to that reported[6] for **9**, but several new reaction sequences were required. The details appear in the manuscript submitted for publication.[5] The ^{1}H-NMR spectrum of tetrad **8** featured resonances for the carotenoid and diquinone moieties that were at similar chemical shifts to those in unlinked model compounds, or slightly downfield of those in the models. These results are consistent with a "linear" conformation in which the carotenoid and diquinone are extended out, away from the porphyrin. Such a conformation is consistent with the partial double bond nature of the amide bonds, which are expected to preclude folded arrangements.

Electrochemistry. Cyclic voltammetric measurements were performed on a model diquinone in order to obtain data for estimation of the energies of charge-separated states. The first and second one-electron reduction potentials in 1,2-dichloroethane were -0.91 V and -1.14 V relative to internal ferrocene. Using these values and those reported previously for carotenoid and porphyrin model compounds, energies of 1.69, 1.46, 1.39 and 1.16 eV are estimated for the C-P$^{\bullet+}$-Q$_A^{\bullet-}$-Q$_B$, C-P$^{\bullet+}$-Q$_A$-Q$_B^{\bullet-}$, C$^{\bullet+}$-P-Q$_A^{\bullet-}$-Q$_B$, and C$^{\bullet+}$-P-Q$_A$-Q$_B^{\bullet-}$ charge-separated states of **8**.

The reduction potentials for the quinone moiety of tetrad **9** were previously reported[6] to be -0.86 and -1.05 V relative to internal ferrocene when determined under similar conditions. Thus, the energies of the C-P$^{\bullet+}$-Q$_A^{\bullet-}$-Q$_B$, C-P$^{\bullet+}$-Q$_A$-Q$_B^{\bullet-}$, C$^{\bullet+}$-P-Q$_A^{\bullet-}$-Q$_B$, and C$^{\bullet+}$-P-Q$_A$-Q$_B^{\bullet-}$ charge-separated states of **9** are estimated to be 1.60, 1.41, 1.30 and 1.11 eV, respectively, as shown in Scheme V. This Scheme will be used to discuss the photochemistry of both **8** and **9**.

Absorption spectra. The absorption spectrum of **8** in dichloromethane (Figure 2) features the porphyrin Soret at 420 nm and Q-band absorptions at 550, 592 and 652 nm. The fourth Q-band (at ~518 nm) is obscured by the carotenoid absorption, which has maxima at 478 and 512 nm. In the UV, a benzoquinone absorption is visible at ~250 nm. The spectrum is essentially a linear combination of the absorption spectra of the component chromophores in model systems, and the spectrum in chloroform is virtually identical to that in dichloromethane.

Figure 2

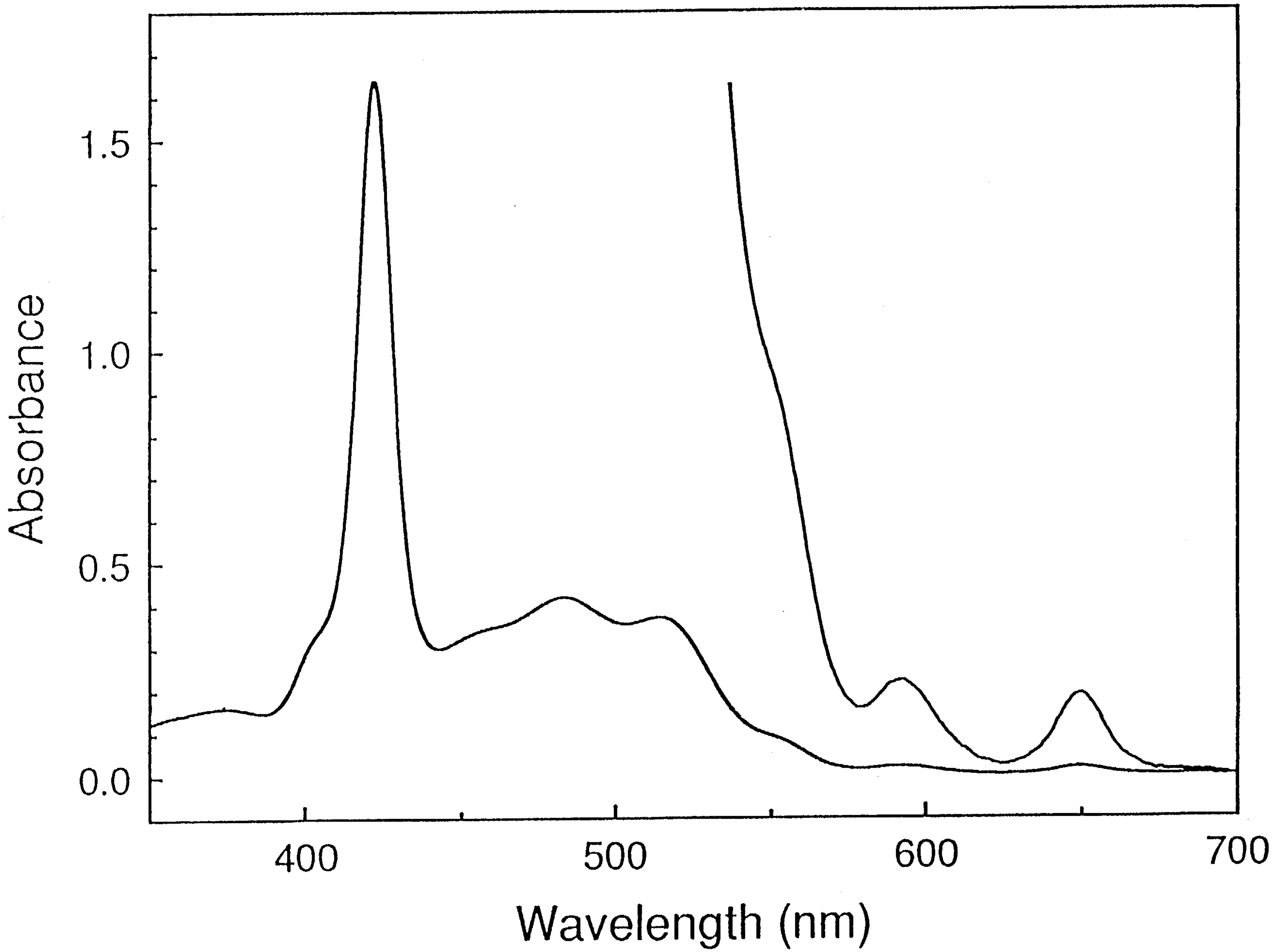

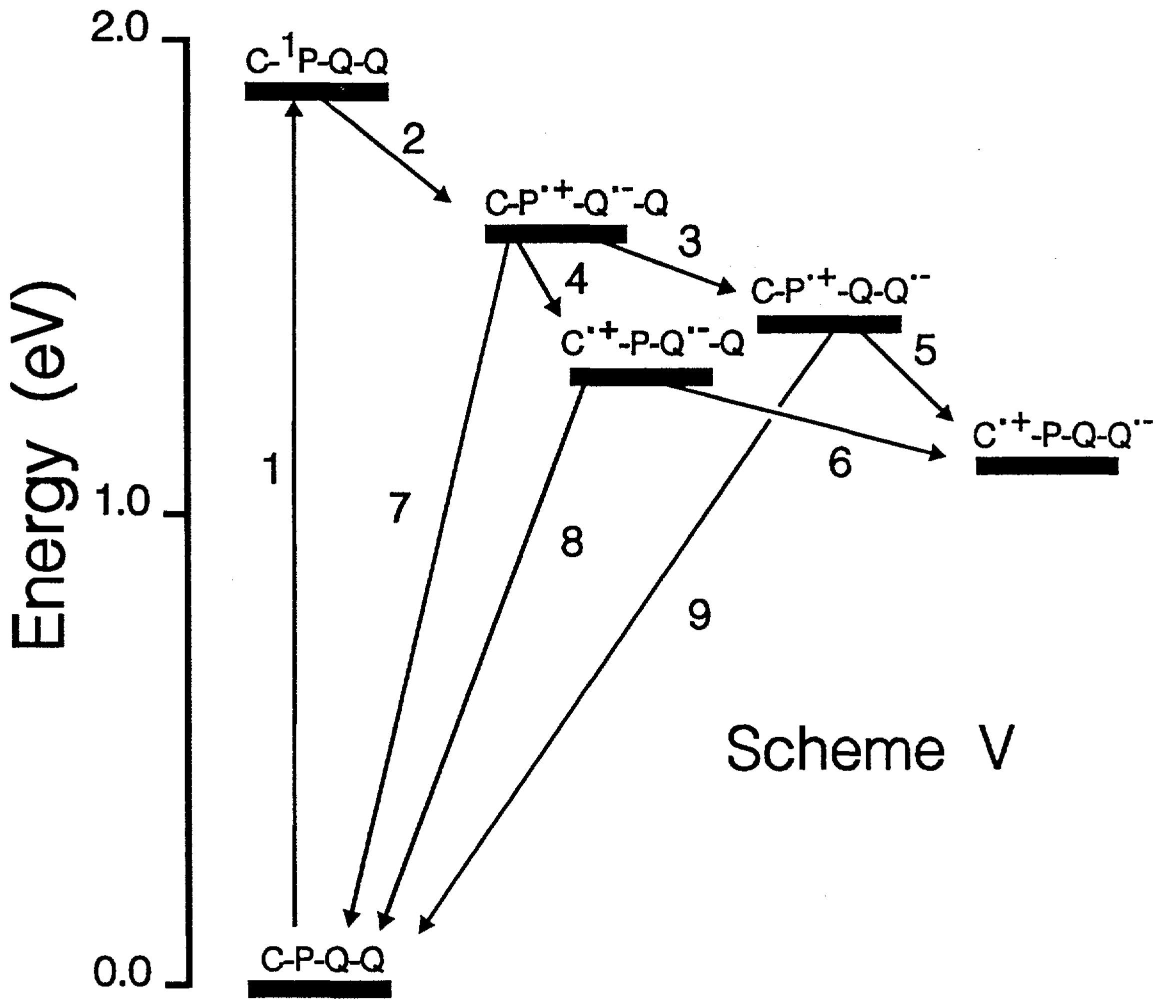

Scheme V

Fluorescence emission spectra. The emission spectrum obtained upon excitation of **8** in dichloromethane at 590 nm consists of a typical tetraarylporphyrin emission with maxima at 655 and 720 nm, but the intensity is much reduced relative to that for a model porphyrin. This quenching is attributed to electron transfer from C-^{1}P-Q_A-Q_B to yield C-$P^{\bullet+}$-$Q_A{}^{\bullet-}$-Q_B (step 2 in Scheme V). Similar results were obtained in chloroform. Quantitative information concerning the degree of quenching was obtained using time-resolved techniques. These studies were carried out using the single photon timing method with excitation at 590 nm. Emission decays were measured for a ca. 1×10^{-5} M solution of **8** in dichloromethane at nine wavelengths in the 645 - 740 nm region. The decays at all these wavelengths were analyzed globally as the sum of four exponential processes (χ^2 = 1.19), and the resulting amplitude and lifetime data at each wavelength were scaled to the corrected steady-state emission spectrum to obtain the decay-associated spectrum shown in Figure 3. The decay at all wavelengths consists of a major component with a lifetime of 0.38 ns and three minor components which may represent impurities or minor conformers.

A suitable model carotenoporphyrin dyad has a porphyrin singlet lifetime of 3.4 ns in dichloromethane. Thus, the 0.38 ns lifetime found for $C\text{-}^1P\text{-}Q_A\text{-}Q_B$ is consistent with the strong quenching noted in the steady-state measurement. If we associate this quenching with electron transfer step 2 in Scheme V, the rate constant for photoinitiated electron transfer, k_2, may be calculated to be 2.3×10^9 s^{-1}. The quantum yield of $C\text{-}P^{\bullet +}\text{-}Q_A^{\bullet -}\text{-}Q_B$, Φ_2, equals 0.87.

Similar time-resolved fluorescence studies were carried out with **8** in chloroform solution. Emission decays were measured at eight wavelengths in the 645 - 740 nm region. The decays at these wavelengths were analyzed globally as four exponential processes ($\chi^2 = 1.15$). The decay at all wavelengths consists of a major component with a lifetime of 0.23 ns, ascribed to $C\text{-}^1P\text{-}Q_A\text{-}Q_B$, and three minor components. The porphyrin excited singlet state lifetime of a suitable model compound in chloroform is 3.5 ns. These data yield a rate constant for photoinitiated electron transfer, k_2, of 4.1×10^9 s^{-1}. The quantum yield of $C\text{-}P^{\bullet +}\text{-}Q_A^{\bullet -}\text{-}Q_B$ is 0.94.

Tetrad **9** demonstrates more rapid photoinduced electron transfer from the porphyrin excited singlet state to the attached quinone than was observed for **8**.[5,6] Tetrad **9** in dichloromethane was excited at 590 nm under the conditions described above for **8**. The emission at the fluorescence maximum of 652 nm consisted of a single exponential decay with a lifetime of 15 ps ($\chi^2 = 1.04$). This lifetime and that of a model compound yield a k_2 value of 6.7×10^{10} s^{-1} and a quantum yield of 1.0 for the $C\text{-}P^{\bullet +}\text{-}Q_A^{\bullet -}\text{-}Q_B$ state. These results are very similar to those mentioned above for pentads **4** and **5**, which feature a similar porphyrin-quinone linkage.

Nanosecond transient absorption spectroscopy. In the above discussion, the quenching of the porphyrin first excited singlet state of **8** by the attached quinone has been interpreted in terms of photoinduced electron transfer to yield a $C\text{-}P^{\bullet +}\text{-}Q_A^{\bullet -}\text{-}Q_B$ charge-separated state. Assuming that this is the case, it is clear from Scheme V that from a thermodynamic point of

Figure 3

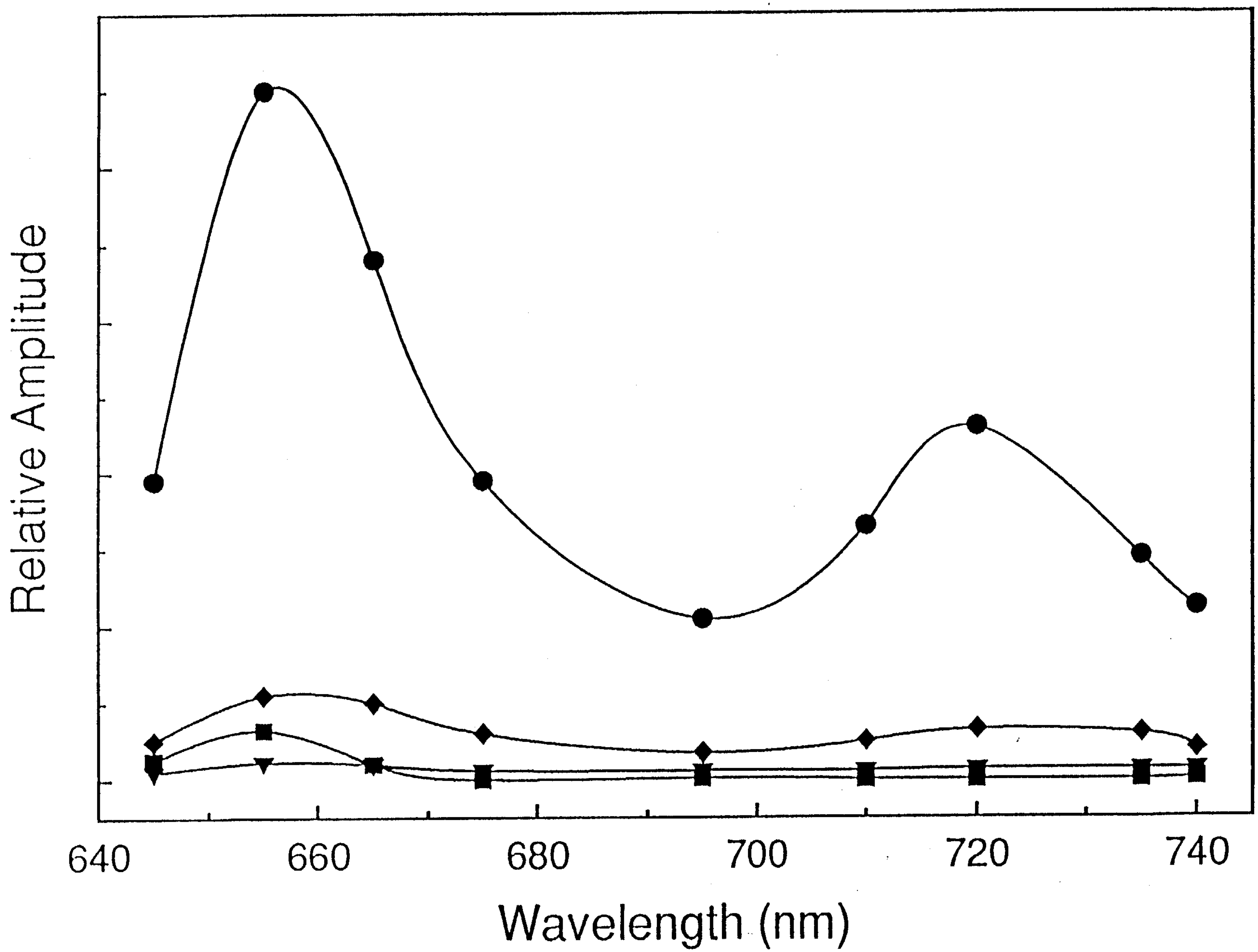

view, this initial state can in principle evolve via steps 3 - 6 to yield a final charge-separated state of the form $C^{\bullet +}$-P-Q_A-$Q_B{}^{\bullet -}$. By analogy with **9**, which produces a similar state with a quantum yield of 0.23 and a lifetime of 460 ns,[5] such a state would be expected to have a relatively long lifetime. Tetrad **8** was investigated using transient absorption spectroscopy on the nanosecond time scale in order to evaluate this possibility.

Excitation of **8** in dichloromethane with a 590 nm, ~10-ns laser pulse resulted in the observation of a strong absorption at 970 nm ascribed to the carotenoid radical cation, which is the only species in such molecules that has significant absorption at this wavelength. This transient is due to the $C^{\bullet +}$-P-Q_A-$Q_B{}^{\bullet -}$ charge-separated state. The decay was fit as a single exponential with a floating baseline to yield a lifetime for $C^{\bullet +}$-P-Q_A-$Q_B{}^{\bullet -}$ of 7.4 μs. The quantum yield of $C^{\bullet +}$-P-Q_A-$Q_B{}^{\bullet -}$ was estimated by the comparative method as 0.49. Similar studies were carried out in chloroform. In this case, the transient absorption of the carotenoid radical cation decayed exponentially in 740 ns, and the quantum yield of $C^{\bullet +}$-P-Q_A-$Q_B{}^{\bullet -}$ was 0.57.

Discussion. These results indicate that although the basic photochemistry of tetrad **8** is similar to that observed for the closely-related **9**, the alteration of the linkage between the porphyrin and quinone moieties has had a substantial effect on the quantum yield and lifetime of the final $C^{\bullet +}$-P-Q_A-$Q_B{}^{\bullet -}$ charge-separated state. The new linkage has reduced the rate of photoinitiated electron transfer step 2 by a factor of about 30. Much of this reduction may be attributed to reduced electronic coupling between the porphyrin and the quinone, although the 0.09 eV decrease in reaction exergonicity also contributes. However, this change only reduces the quantum yield of step 2 by about 10%, to 0.87, as expected from the discussion in the introduction of this report. Changing the solvent to chloroform, increases the rate of step 2 in **8** by a factor of about two, and this raises the quantum yield to 0.94.

In spite of the reduction in the quantum yield of step 2 in **8** relative to **9**, the quantum yield of the final state of **8** in dichloromethane is about twice that for **9** in the same solvent. This must be the result of a different balance among the rates of steps 3 - 9 in Scheme V. The efficiency of steps 3 - 6 in tetrad **9** in dichloromethane equals the quantum yield of $C^{\bullet +}$-P-Q_A-$Q_B^{\bullet -}$ divided by that for C-$P^{\bullet +}$-$Q_A^{\bullet -}$-Q_B, or 0.23. In tetrad **8** in the same solvent, the efficiency is 0.56. In chloroform, the efficiency of steps 3 - 6 increases to 0.61. The simplest explanation for the difference in quantum yield of the final state between **9** and **8** is a change in the partitioning of C-P $^{\bullet +}$-$Q_A^{\bullet -}$-Q_B between reaction via steps 3 and 4 and charge recombination by step 7. Because the change in linkage has little effect on the thermodynamic driving force for steps 3 and 4, and electron transfer by these steps does not occur across the porphyrin-quinone linkage, it is reasonable to attribute the increase in efficiency in tetrad **8** mainly to a decrease in the rate of charge recombination by step 7 that accompanies the decrease in the rate of step 2.

The lifetime of the final $C^{\bullet +}$-P-Q_A-$Q_B^{\bullet -}$ state of **8** in dichloromethane is about 16 times longer than that of **9** in the same solvent. A lengthening is consistent with the decreased electronic coupling between the porphyrin and the quinone and the increased separation between them (and between the carotenoid and the quinone). By analogy with other multicomponent systems, it is possible that charge recombination involves a stepwise process, rather than direct migration of an electron from the quinone anion to the carotenoid radical cation.

D. Spectroscopic Studies of Artificial Reaction Centers.

1. Subpicosecond Spectroscopic Studies of Artificial Reaction Centers.

We now have the capability of carrying out transient absorption studies on the subpicosecond time scale, due to the completion of a spectrometer funded in part by the DOE University Instrumentation Program. In principle, this spectrometer allows the study of short-lived intermediates involved in the multistep electron transfer sequences (e.g. Schemes I - V) Molecular devices composed of three components have the minimum level of complexity necessary to permit a multistep electron transfer process leading to a long-lived charge-separated state, and we have therefore begun our picosecond investigations on a molecule of this type. An example is triad **10**, which comprises a free base porphyrin covalently linked to a quinone electron acceptor and a carotenoid electron donor. We have previously reported[8,9] that excitation of the porphyrin moiety of **10** leads to the formation of a charge-separated state $C^{\bullet+}$-P-$Q^{\bullet-}$ that has a lifetime of ~300 ns in dichloromethane solution and several μs in acetonitrile. The quantum yield is 0.04 in dichloromethane and ~0.25 in the same solvent saturated with tetra-*n*-butylammonium tetrafluoroborate. Studies of suitable model compounds suggested that the long-lived $C^{\bullet+}$-P-$Q^{\bullet-}$ charge-separated state was formed by a two-step electron transfer sequence. The porphyrin first excited singlet state C-^{1}P-Q decays by electron transfer to the attached quinone to yield C-$P^{\bullet+}$-Q $^{\bullet-}$, and the carotenoid then donates an electron to the porphyrin radical cation to yield the final species. However, information about the rates of formation and decay of the intermediate state was lacking. We have now completed a study of photoinitiated electron transfer in triad **10** in benzonitrile solution on the picosecond time scale that yields information concerning the formation and decay of the intermediate charge-separated state. The results have recently been submitted for publication.[10]

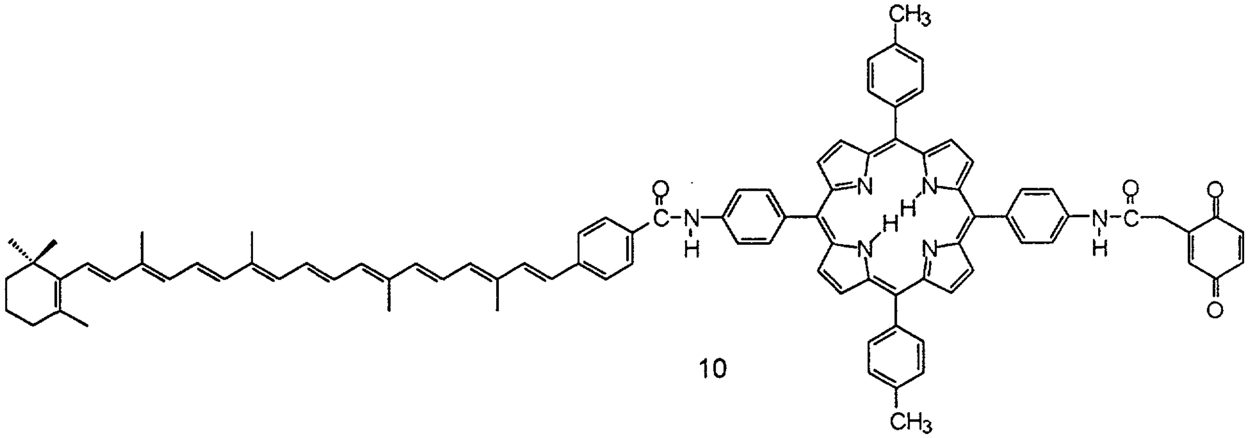

10

Fluorescence decay studies. Excitation of the porphyrin moiety of **10** in benzonitrile gives rise to a typical tetraarylporphyrin emission spectrum with maxima at 659 and 725 nm. This emission is strongly quenched relative to that of model porphyrins or carotenoporphyrins. The kinetics of the quenching process were studied using the singlet photon timing technique. The porphyrin moiety of **10** was excited at 590 nm and the fluorescence decay measured at 10 wavelengths in the 640 - 745 nm region. The data were analyzed globally as the sum of 3 exponentials (χ^2 = 1.16). The major component of the decay has a lifetime of 0.34 ns, and represents the decay of C-^{1}P-Q.

A model porphyrin has a singlet excited state lifetime of ~10 ns under the same conditions, whereas the porphyrin fluorescence of model carotenoporphyrin **11** decays with a lifetime of 2.2 ns The much shorter lifetime of the porphyrin first excited singlet state in **10** shows that attachment of the quinone to the carotenoporphyrin has opened a new decay pathway which is assigned to electron transfer from the porphyrin to the quinone to generate the C-P$^{\bullet+}$-Q$^{\bullet-}$ charge-separated state. Similar electron transfer has been observed in a large number of porphyrin-quinone dyad systems. The rate constant for this electron transfer, k_1, is calculated to be 2.4 × 10^9 s^{-1} and the quantum yield of C-P$^{\bullet+}$-Q$^{\bullet-}$is 0.82.

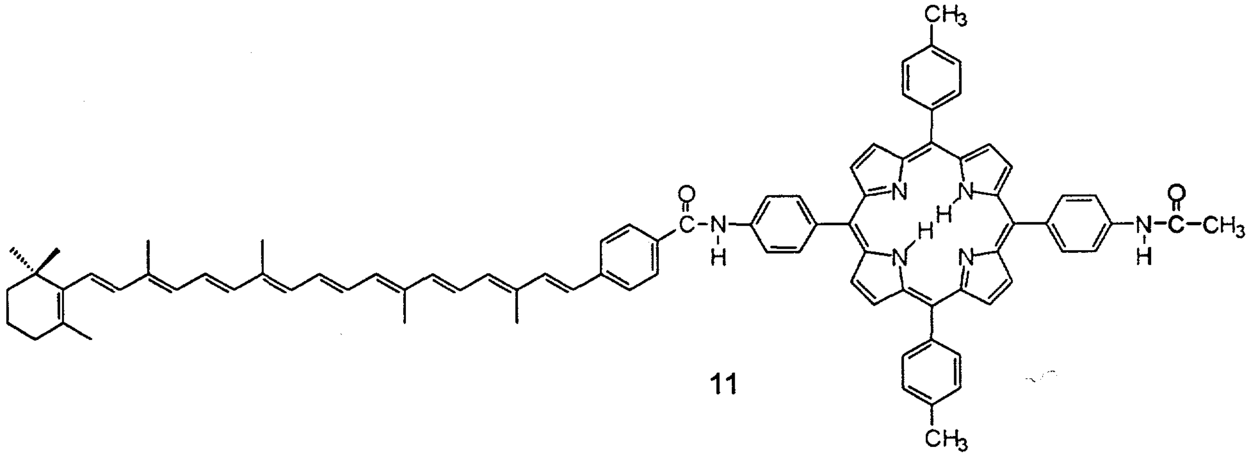

11

Fluorescence decay results for model porphyrin-quinone **12** are consistent with this interpretation. The porphyrin moiety of **12** in benzonitrile was excited with a 590-nm laser pulse, and the fluorescence decay was measured at 655 and 720 nm. The decays at both wavelengths consisted of a major component with a lifetime of 0.47 ns that is ascribed to decay of ^{1}P-Q. Analysis of this data yields an electron transfer rate constant of 2.0 × 10^9 s^{-1}, which is very close to that determined above for **10**. Attachment of the carotenoid does not significantly affect the rate of porphyrin-quinone electron transfer. The quantum yield of P$^{\bullet+}$-Q$^{\bullet-}$ in **12** is 0.94.

The fluorescence decay studies for carotenoporphyrin **11** show some quenching of the porphyrin first excited singlet state by the carotenoid. Possible mechanisms for this quenching will be discussed later. The rate constant for this quenching process, $k_{1'}$, is 3.6×10^8 s^{-1}. It is reasonable to assume that this quenching would also be a minor decay process for the porphyrin first excited singlet state of triad **10**. If we assume that the rate is unchanged by attachment of the quinone moiety to the carotenoporphyrin, then the quantum yield of this quenching process in the triad is $k_{1'} \times \tau_{CPQ}$, or 0.12.

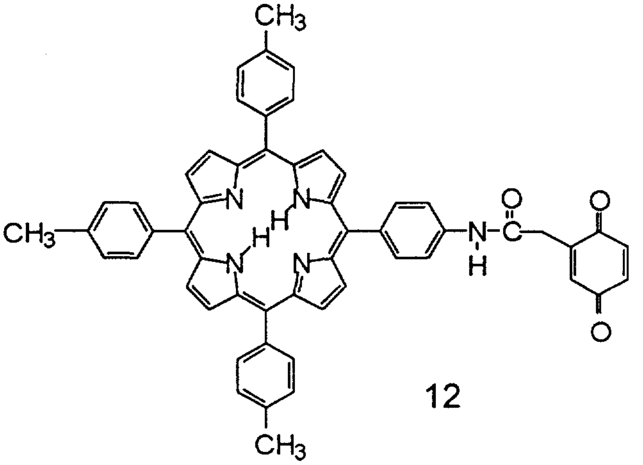

12

Transient absorption studies. The rise and decay of C-P$^{\bullet+}$-Q$^{\bullet-}$ and C$^{\bullet+}$-P-Q$^{\bullet-}$ following excitation of the porphyrin moiety can in principle be measured by the transient absorption changes due to the formation of the porphyrin and carotenoid radical cations. Figure 4 presents the transient spectrum taken 50 ps after excitation at 600 nm of a solution of **10** in benzonitrile with a 150-fs laser pulse. The most prominent features of the spectrum are the stimulated emission bands at 655 and 730 nm that correspond to the fluorescence bands arising from the porphyrin first excited singlet state. Kinetic analysis at the minima of these bands is not possible because the net absorption change is near zero. However, at 700 nm there is adequate signal, and the resulting decay is presented in Figure 5. Both the porphyrin radical cation and excited singlet species are known to absorb in this region. The rise time of the transient was not resolved on this time scale; its decay time was 0.34 ns. The dominant feature of the transient spectrum in the near IR of the same sample is the absorption of the carotenoid radical cation centered at 955 nm. This transient has a rise time of 0.34 ns (Figure 6) and decays with a lifetime of 370 ns. From the maximum δA, the yield of C$^{\bullet+}$-P-Q$^{\bullet-}$ was calculated to be 0.13.

Figure 4

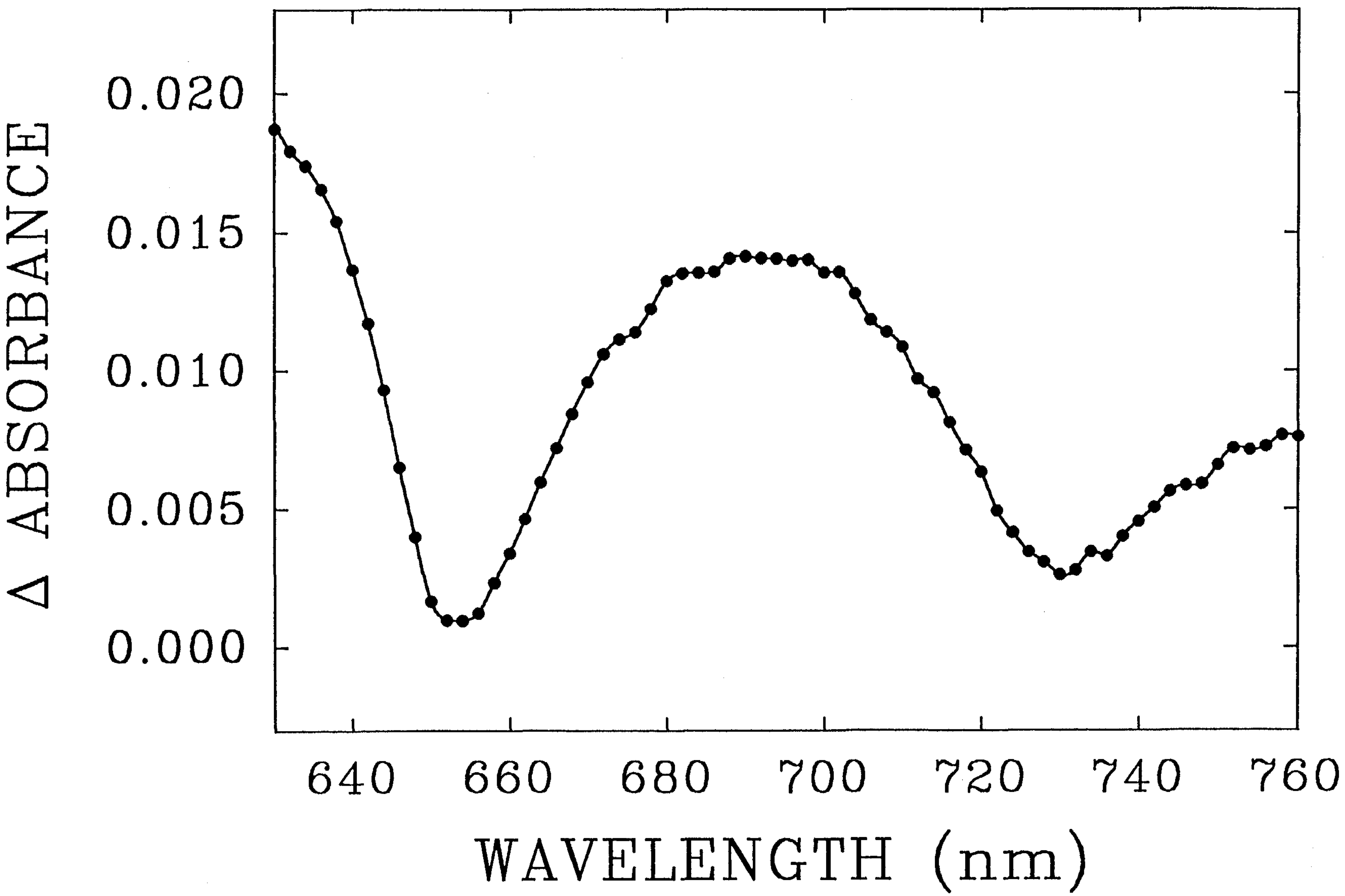
0.020
0.015
0.010
0.005
0.000
Δ ABSORBANCE
640
660
680
700
720
740
760
WAVELENGTH (nm)

Figure 5

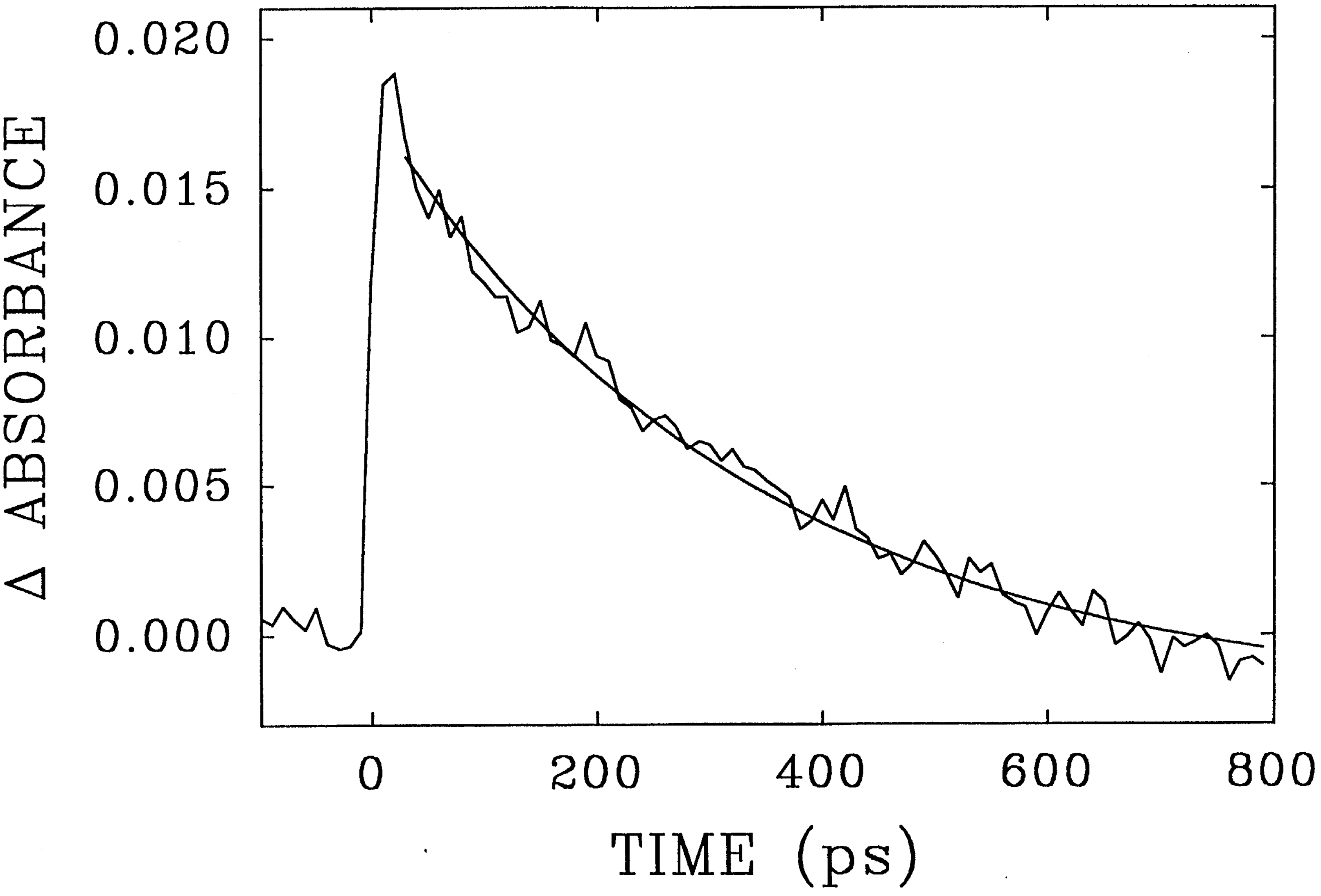
0.020
0.015
0.010
0.005
0.000
Δ ABSORBANCE
0
200
400
600
800
TIME (ps)

Figure 6

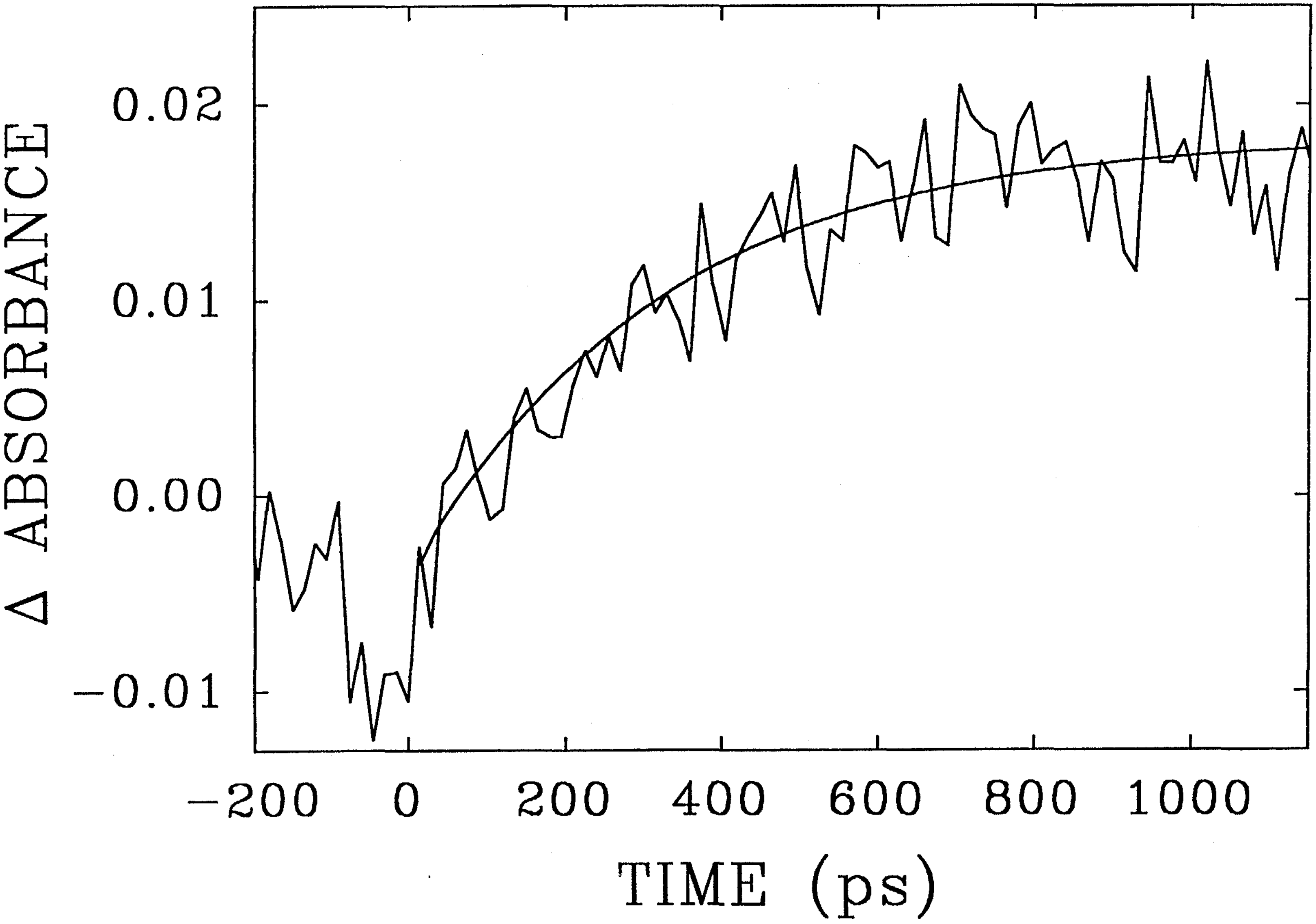

Because the transient absorption of the carotenoid radical cation rises with the same time constant as the decay of the porphyrin first excited singlet state, any intermediate in the formation of $C^{\bullet +}$-P-$Q^{\bullet -}$ from C-^{1}P-Q must have a short lifetime. In order to investigate this possibility, subpicosecond transient absorption studies with excitation at 600 nm were also carried out on porphyrin-quinone dyad **12** in benzonitrile. Figure 7 shows the decay of the transient absorption at 680 nm and Figure 8 presents the rise of the same signal on a shorter time scale. These data were fit as the sum of two exponentials to yield a rise time of ca. 1.5 ps and a decay of 0.46 ns. Although the rise in Figure 8 was observed consistently in several samples, the signal-to-noise ratio is poor, and the rise time quoted above can only be considered a rough estimate. Thus, the transient absorption of dyad **12** at 680 nm decays with essentially the same time constant as the fluorescence of the ^{1}P-Q state, and rises on a much faster time scale.

Discussion. The fluorescence data show that the C-^{1}P-Q excited singlet state of triad **10** in benzonitrile decays by both a major pathway with a quantum yield of 0.82 and a minor pathway with a yield of 0.12. Each of these decay routes will be discussed in turn.

Major decay pathway. Scheme VI shows some of the conceivable decay pathways for **10** and the related excited and charge-separated states. Because the major decay pathway for the porphyrin first excited singlet state of **10** is observed only upon linking the quinone to the carotenoporphyrin moiety, it is clear that it concerns the right-hand set of electron transfer steps in the Figure (steps 1 - 4). The initial event is photoinduced electron transfer from C-^{1}P-Q to yield C-$P^{\bullet +}$-$Q^{\bullet -}$(step 1). This step can also be studied in the simpler porphyrin-quinone model **12**, and results for this molecule will be discussed first.

As mentioned above the rate constant for photoinduced electron transfer, k_1, for dyad **12** is 2.0×10^9 s^{-1}. The transient absorption of **12** at 680 nm decays with essentially the same lifetime, even though the porphyrin radical cation of $P^{\bullet +}$-$Q^{\bullet -}$ absorbs significantly at this wavelength. Why is a longer-lived charge-separated state not observed, and what is the source of the fast-rising component of the transient absorption in Figure 8? A reasonable explanation for this observation is inherent in eq 1, which is the expression governing the concentration of

Figure 7

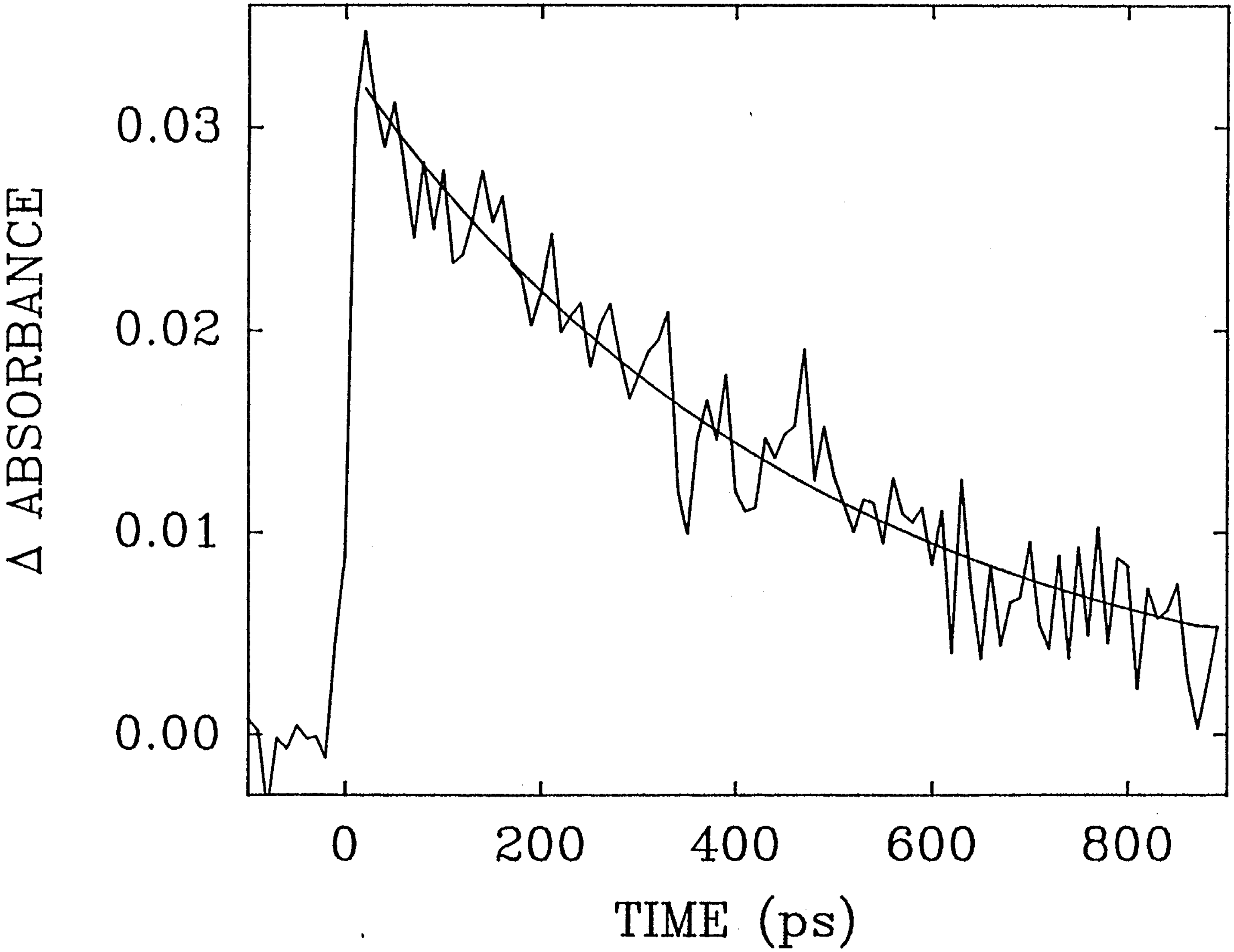

Figure 8

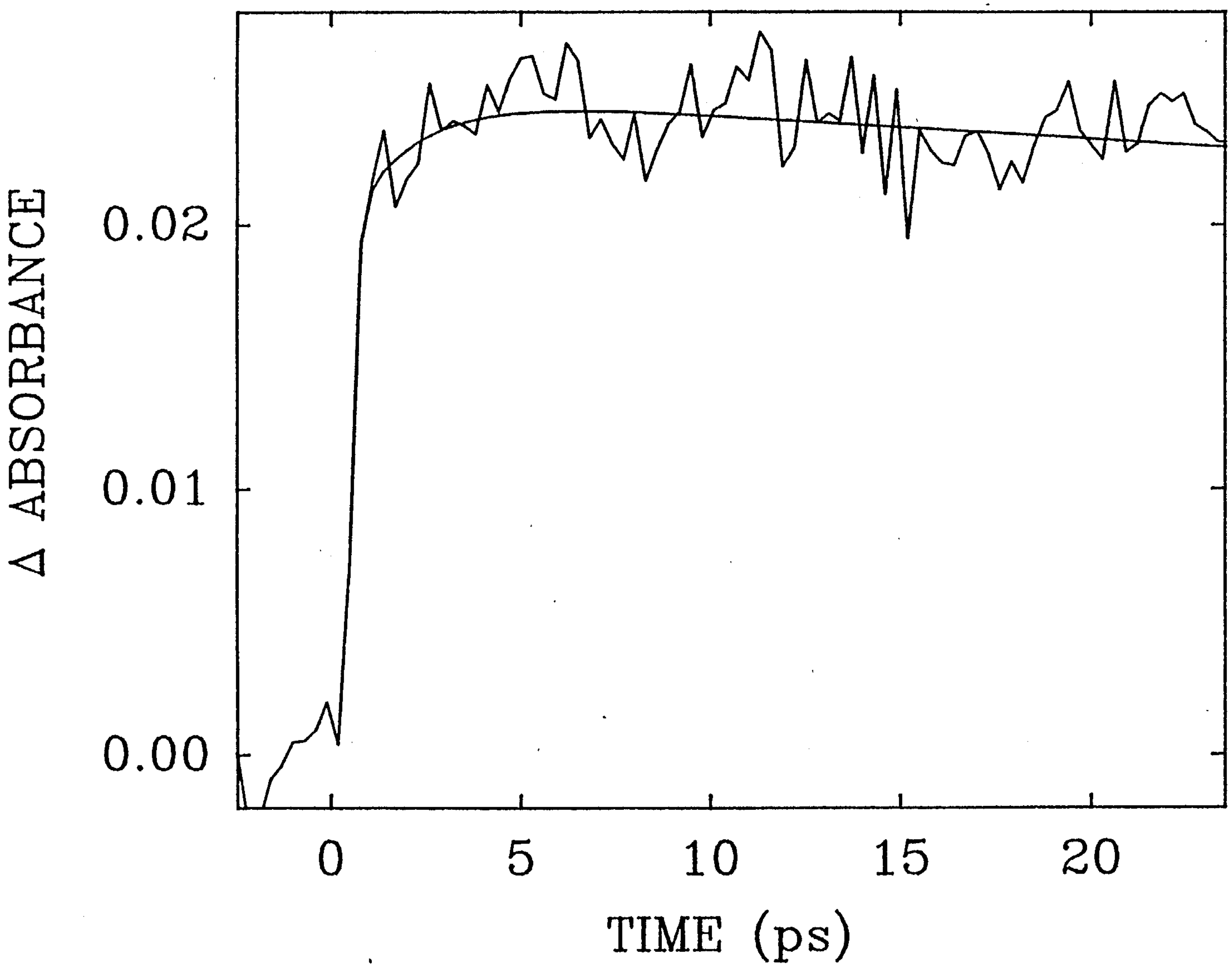

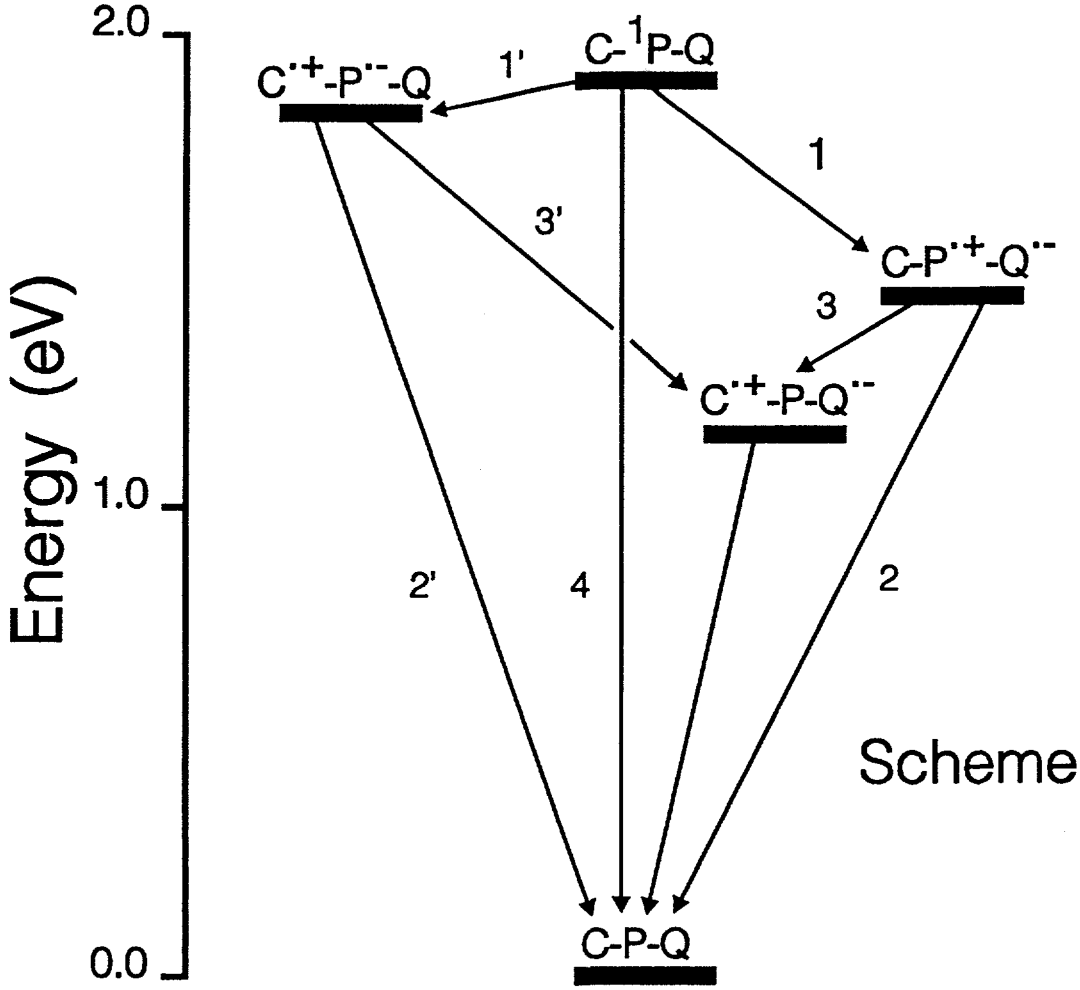

Scheme VI

$P^{\bullet+}$-$Q^{\bullet-}$ as a function of time after laser excitation, where k_2 is the rate

$$[P^{\bullet+} - Q^{\bullet-}] = k_1[^1P - Q]_0(k_2 - k_1)^{-1}(e^{-k_1 t} - e^{-k_2 t}) \qquad (1)$$

of charge recombination to the ground state (analogous to step 2 in Scheme VI) and t is the time after formation of the porphyrin first excited singlet state with an initial concentration of $[^1P\text{-}Q]_0$. It is apparent that the greater of k_1 or k_2 will appear as the rise time constant of the transient. From the fluorescence decay of **12**, k_1 is unambiguously assigned to the formation of $P^{\bullet+}$-$Q^{\bullet-}$, even though it appears as the time constant for the decay of the transient absorption at 680 nm. Therefore, the rise time of the transient must be associated with the rate constant k_2 for the *decay* of $P^{\bullet+}$-$Q^{\bullet-}$. In other words, k_2 is greater than k_1, and the rise of the $P^{\bullet+}$-$Q^{\bullet-}$ transient absorption in Figure 8 is kinetically controlled by the decay constant for $P^{\bullet+}$-$Q^{\bullet-}$, whereas the decay in Figure 7 is controlled by the decay of ^{1}P-Q. From the rough estimate for the rise time of 1.5 ps, k_2 is calculated to be about 7×10^{11} s^{-1}. The decay rate of P$^{\bullet+}$-Q$^{\bullet-}$ is much faster than its formation rate in this solvent.

Turning now to the results for triad **10**, Scheme VI indicates that the product of the major quenching pathway for the porphyrin first excited singlet state is C-P$^{\bullet+}$-Q$^{\bullet-}$, whose concentration as a function of time is given by eq 2.

$$[\mathrm{C}\text{-}\mathrm{P}^{\bullet+}\text{-}\mathrm{Q}^{\bullet-}] = k_1[\mathrm{C}\text{-}^1\mathrm{P}\text{-}\mathrm{Q}]_0((k_2+k_3)-(k_1+k_4))^{-1}(e^{-(k_1+k_4)t}-e^{-(k_2+k_3)t}) \tag{2}$$

Eq 3 gives the time dependence of the rise of the final C$^{\bullet+}$-P-Q$^{\bullet-}$ charge-separated state.

$$[\mathrm{C}^{\bullet+}\text{-}\mathrm{P}\text{-}\mathrm{Q}^{\bullet-}] = k_1[\mathrm{C}\text{-}^1\mathrm{P}\text{-}\mathrm{Q}]_0((k_2+k_3)-(k_1+k_4))^{-1}(e^{-(k_1+k_4)t}-e^{-(k_2+k_3)t})e^{k_2 t} \tag{3}$$

The slow decay of the final state is not considered in this equation.

The spectroscopic data discussed above show that in **10** the transient absorption at 700 nm (Figure 5), ascribed to C-^{1}P-Q and C-P$^{\bullet+}$-Q$^{\bullet-}$, decays with the 0.34 ns lifetime of the porphyrin first excited state, as monitored by fluorescence lifetime studies. Similarly, the C$^{\bullet+}$-P-Q$^{\bullet-}$ state rises with this same lifetime. Examination of eq 2 and 3 shows that this is expected when k_2 and k_3 in Scheme VI are much larger than k_1 plus k_4, so that decay of C-^{1}P-Q is the rate-limiting step in the formation of C$^{\bullet+}$-P-Q$^{\bullet-}$. Under these conditions, the rise kinetics of C$^{\bullet+}$ -P-Q$^{\bullet-}$ are essentially transparent to the decay of C-P$^{\bullet+}$-Q$^{\bullet-}$ by k_2 and k_3, although the relative rates of these steps do of course affect the yield.

Although the yield of photoinduced electron transfer step 1 in triad **10** is 0.82, the yield of the final C$^{\bullet+}$-P-Q$^{\bullet-}$ state is only 0.13. Thus, k_2, the rate constant for charge recombination of C-P$^{\bullet+}$-Q$^{\bullet-}$ by step 2, must be substantially larger than k_3, which represents electron donation from the carotenoid to the porphyrin radical cation. Quantitatively, the overall yield of the final state, $\Phi_{\mathrm{C}^{\bullet+}\text{-P-Q}^{\bullet-}}$, is given by eq 4.

$$\Phi_{C^{\bullet+}\text{-P-Q}^{\bullet-}} = (\Phi_{\text{C-P}^{\bullet+}\text{-Q}^{\bullet-}})(k_3 / (k_2 + k_3)) \qquad (4)$$

It is possible to calculate a value for k_3 of 1×10^{11} s^{-1} based on the quantum yields of $C^{\bullet+}$-P-$Q^{\bullet-}$ and C-$P^{\bullet+}$-$Q^{\bullet-}$ and the value of k_2 estimated from the results for porphyrin-quinone dyad **12**.

Examination of eqs 2 and 3 shows that although the formation of $C^{\bullet+}$-P-$Q^{\bullet-}$ from C-^{1}P-Q is not in general a simple exponential process, under the conditions where k_2 and k_3 are both substantially larger than k_1 and k_4, the rise time of $C^{\bullet+}$-P-$Q^{\bullet-}$ will be governed by $k_1 + k_4$ beginning a few ps after excitation. Indeed kinetic simulation of the major decay process in Scheme VI using the values for k_1 through k_4 given above yields a rise of $C^{\bullet+}$-P-$Q^{\bullet-}$ that is indistinguishable from an exponential process with a 0.34 ns time constant (Figure 6).

Minor decay pathway. In benzonitrile, the quantum yield of C-$P^{\bullet+}$-$Q^{\bullet-}$ from C-^{1}P-Q is 0.82, and thus decay of the porphyrin first excited singlet state also occurs by other pathways. Some of these are porphyrin internal conversion, intersystem crossing and fluorescence. However, it was mentioned above that C-^{1}P-Q also decays by a minor pathway with a quantum yield of 0.12, based on the 2.2 ns lifetime of C-^{1}P in model carotenoporphyrin **11**. What is the nature of this carotenoid quenching of the porphyrin first excited singlet state?

One possibility is singlet energy transfer from C-^{1}P to yield the "forbidden" carotenoid A_g state, ^{1}C-P. Evidence for quenching by such an energy transfer process has recently been reported in carotenoporphyrins in which the carotenoid and porphyrin moieties are more tightly coupled electronically than is the case for **10** and **11**. A second possibility for the minor quenching is electron transfer from the carotenoid polyene to the porphyrin first excited singlet state to yield $C^{\bullet+}$-$P^{\bullet-}$-Q ($k_{1'}$ in Scheme VI). This process is estimated to be exergonic, although the thermodynamic driving force is very small (0.07 eV, Scheme VI). As the quantum yield of the minor quenching pathway is 0.12 and the yield of the final $C^{\bullet+}$-P-$Q^{\bullet-}$ state in **10** is 0.13 in benzonitrile, such electron transfer quenching could in principle contribute significantly to the yield of $C^{\bullet+}$-P-$Q^{\bullet-}$ in this solvent via the electron transfer pathways shown on the left-hand side of Scheme VI (steps 1' and 3'). Although we have discussed this possibility in previous reports, several studies of **11** and related carotenoporphyrins have produced no evidence for a $C^{\bullet+}$-$P^{\bullet-}$ state. Recently, however, we have reported transient absorption results for a new carotenoporphyrin, in which the porphyrin moiety bears three pentafluorophenyl groups.[3] These groups strongly stabilize the porphyrin radical anion, and as a result the formation of $C^{\bullet+}$-$P^{\bullet-}$ in this molecule from C-^{1}P is exergonic by 0.42 eV. In addition, a modification of the linkage joining the porphyrin and carotenoid moieties favors electron transfer. Excitation of the porphyrin moiety of this compound in butyronitrile solution resulted in the formation of a $C^{\bullet+}$-$P^{\bullet-}$ charge-separated state with a rate constant of 1.8×10^{10} s^{-1} that decayed very rapidly (a rate constant for charge recombination of $\sim 3.3 \times 10^{11}$ s^{-1}).

In light of these new results, it is interesting to consider the possibility that the pathways on the left-hand side of Scheme VI may contribute to the quantum yield of the final charge-separated state in **10**. The small but significant quantum yield for step 1' coupled with the lack of an observable intermediate state in the picosecond data for **10** make it impossible to rule out such a contribution on direct spectroscopic grounds. However, given the quantum yield of only 0.12 for step 1', it is clear that step 3' would have to have to occur substantially faster than step 2' if the yield of the final charge-separated state by this route were to be significant; the rate of step 3' would have to approach 10^{12} s^{-1}.

Although a contribution from steps 1' and 3' to the formation of $C^{\bullet+}$-P-$Q^{\bullet-}$ in **10** in benzonitrile cannot be ruled out due to the relatively slow quenching of C-^{1}P-Q by step 1, possible contributions from a similar mechanism are insignificant in some related multicomponent devices. For example, triad **13**, to be discussed below, has a carotenoporphyrin moiety similar to that in **10**, but the acceptor is based on naphthoquinone. In chloroform solution, the C-^{1}P-Q fluorescence lifetime is only 0.035 ns. The yield of quenching by step 1 in Scheme VI is 0.98, whereas that by step 1' is 0.0067. In this molecule, excitation of the porphyrin moiety leads to production of a final $C^{\bullet+}$-P-$Q^{\bullet-}$ charge-separated state with a quantum yield of 0.07 and a lifetime of 40 ns. Thus, if the minor pathway contributes at all to the formation of the final state, that contribution is less than 10%. Indeed, with triad **10** itself in dichloromethane solution, the yield of the C$^{\bullet+}$-P-Q$^{\bullet-}$ state is 0.04, whereas the quantum yield of porphyrin quenching by the carotenoid is <0.02. An extreme example is provided by C-P-Q-Q molecular tetrad **9**. In dichloromethane solution, the lifetime of the porphyrin first excited singlet state is 15 ps, and the diquinone moiety quenches the C-^{1}P-Q-Q excited state with a quantum yield of unity by a pathway analogous to step 1 in Scheme VI (see Scheme V). Thus, a contribution from carotenoid quenching of the porphyrin first excited singlet state to the quantum yield of 0.23 found for the C$^{\bullet+}$-P-Q-Q$^{\bullet-}$ charge-separated state in this molecule is precluded.

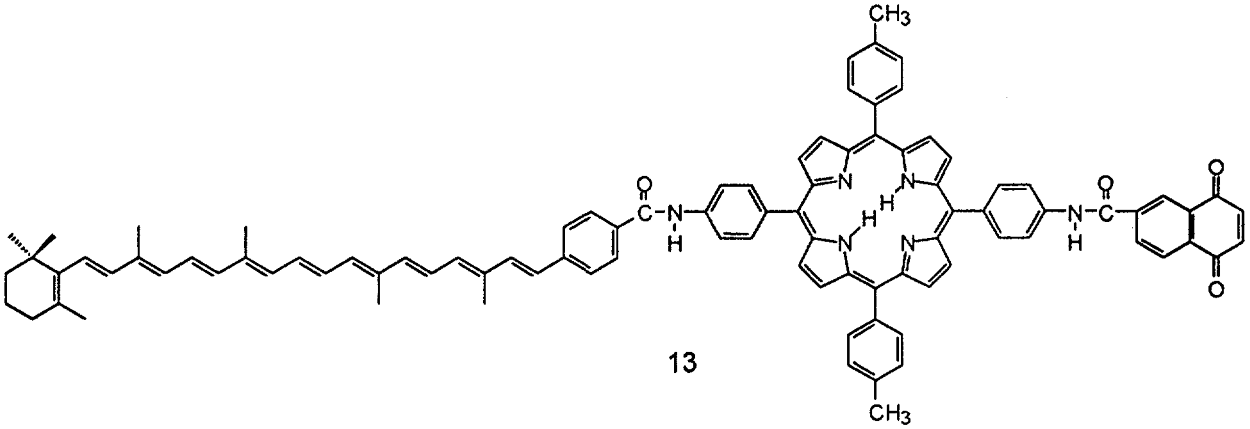

13

Although there is as yet no evidence that this minor pathway does contribute to charge separation in **10**, its existence is an intriguing possibility. If it does play a role, then Scheme VI would be an excellent example of multiple parallel and sequential electron transfer pathways whose convergence enhances the overall yield of a long-lived charge separated species.

2. Time-Resolved EPR Studies of Artificial Reaction Centers.

During this grant period we have continued our collaborative electron paramagnetic resonance studies of the charge-separated states formed by excitation of artificial reaction centers. The spectroscopic group is led by J. R. Norris, H. Levanon, and M. Bowman. The studies thus far have focused on tetrad 9 in dichloromethane. Intramolecular electron transfer from the C-^{1}P-Q-Q excited singlet state was studied by selective laser excitation with both Fourier transform and CW-EPR spectroscopies. It was found that the electron transfer occurs from the singlet state of the porphyrin to produce the terminal benzoquinone radical anion and the carotenoid radical cation (Scheme V). It was possible to observe and identify both the quinone radical anion and the carotenoid radical cation, to verify the excited singlet state as the precursor, and to observe weak electronic coupling between the radical ions which verified the intramolecularity of the reactions.

The EPR spectra obtained from CW-EPR spectroscopy using pulsed laser excitation depend strongly on the time interval between the laser pulse and the position of the detection window of the transient magnetization profile. This may lead to misinterpretation of the radical intermediates participating in the reaction routes. Spectral distortions arise from small hyperfine splittings and narrow line widths, resulting in the appearance of Torrey wiggles at off-resonance fields. The correct spectrum, however, with the correct line shape appears at times above 1 μs after the laser pulse, and is in complete agreement with the Fourier transform EPR spectrum. Analysis and reconstruction of the transient spectra were carried out in Fourier conjugate space. The experimental CW spectra were shown to be the Fourier transform of the free-induction decay multiplied by an appropriate windowing function. The changes in the spectra taken less than 1 μs after excitation are due to line distortions and not to chemical processes. Although these conclusions were derived from the studies of tetrad **9**, the treatment is of general applicability in the analysis of time-resolved CW-EPR spectra.

The results of the EPR studies have appeared in the *Journal of the American Chemical Society*[11] and *Applied Magnetic Resonance.*[12]

3. Photoacoustic Studies of Artificial Reaction Center Components.

In the studies by this research group mentioned above and by other groups in this general research area, the energies of the various charge-separated states are usually estimated from cyclic voltammetric studies of the molecules in question or model compounds. This is necessary because the charge-separated states are non-emissive, so that the energies cannot be determined spectroscopically. Occasionally, it has been possible to estimate the energies of high-lying states through observation of an equilibrium with emissive excited states, but this method is not generally applicable. Photoacoustic spectroscopy is in principle capable of measuring the energies of spectroscopically silent transient states. We have been investigating this possibility using the carotenoid triplet state, whose energy was previously unknown, as a model.

The energy of the lowest triplet excited state of a carotenoid polyene. The lowest-energy electronic excited state in the chromophores of photosynthetic membranes and in the synthetic reaction centers discussed in this report is that of the carotenoid polyenes. Although the carotenoid triplet species is central to photoprotection and is populated in a variety of spectroscopic experiments on photosynthetic preparations, the energy gap between the lowest triplet and the carotenoid ground state is not known.

Previous attempts to determine the carotenoid triplet energy have involved several different approaches. The most straightforward measurement would be to detect the phosphorescence and to record its spectrum. This has proven futile in isolated carotenoids in solution because the quantum yield of intersystem crossing is vanishingly small so that the triplet state is not populated by excitation into the singlet manifold. Sensitization by a triplet donor ordinarily requires diffusion and collisions which are precluded in the frozen glassy matrix required to enhance phosphorescence. In order to overcome this obstacle, we have attempted to detect phosphorescence from the carotenoid moiety of carotenoporphyrin dyads in which triplet sensitization is intramolecular and in which the triplet yield is greater than 50% in frozen glasses. No signal was observed in the wavelength range 600 to 1300 nm.

A second traditional technique used in organic photochemistry to locate optically unobservable triplet states is to do a series of quenching experiments with triplet energy donors of descending energy. When the donor triplet energy is significantly lower than that of the unknown, the quenching rate constant will decrease abruptly and thus the unknown triplet energy can be bracketed between two known energies. These experiments have failed with carotenoid polyenes, apparently because no donor could be found with an energy low enough to attenuate the quenching rate constant.

We have carried out experiments using sensitive time-resolved singlet oxygen detection and have found that no detectable singlet oxygen is produced by the triplet of a carotenoid linked to a porphyrin sensitizer. One interpretation of this result is that the equilibrium

$$^3\text{C-P} + \text{O}_2 \;=\; {}^1\text{O}_2 + \text{C-P}$$

lies far to the left, with ^{3}C being less that ca. 0.8 eV.

Another approach to determining the triplet energy involves measuring the O_2 perturbed ground state to excited triplet state absorption spectrum. Although this is an interesting experiment, the results are necessarily equivocal in that the optical transition could be from the ground state to any upper triplet state, not necessarily the lowest one. Truscott has attempted these experiments but has not reported significant results.

In order to measure the lowest triplet energy of a carotenoid polyene, we have now used laser flash photoacoustic spectroscopy to measure the thermal energy which accompanies the relaxation of ^{3}C-P in a carotenoporphyrin dyad in solution. Briefly, after flash excitation of a C-P dyad to produce C-^{1}P, relaxation to C-P and ^{3}C-P produces an "instantaneous" (ns) thermal expansion in the solution. This expansion launches an acoustic wave which is detected by a piezoelectric transducer (PZT) oscillating at its fundamental frequency. The thermal energy generated by the process $^3\text{C-P} \rightarrow \text{C-P}$ also causes a thermal expansion in the solution which generates an acoustic wave, but the heat source for this wave is not instantaneous. It has the time dependence of the triplet relaxation process which determines the triplet lifetime of the carotenoid. The arrival of the wave generated by the slower heat source at the PZT produces oscillations having different amplitudes and phases from those produced by the instantaneous or fast heat. Analysis of the data involves reconstructing the observed oscillations as a linear combination of a fast heat source component and a slow heat source component and identifying the slow heat source component with the fraction of decay to form ^{3}C-P (triplet quantum yield) and the energy of the ^{3}C-P species.

Experimentally, a cell was constructed with a PZT attached to the side, and provisions were included for changing the sample without moving the optical assembly. Laser flash excitation and digital collection of the PZT signal was performed with our conventional ns flash spectrometer. The sample selected for these experiments was a *para*-linked carotenoporphyrin similar to **11**. In order to calibrate the system an oxygen-saturated solution of this carotenoporphyrin was excited and the resulting oscillations of the PZT recorded. This signal is labeled S_{quenched}, and serves as an all-fast heat source because ^{3}C-P is quenched to C-P by oxygen (without sensitization of singlet oxygen) within 50 ns (which is instantaneous on the time scale of our PZT (f_o = 160 kHz)). The oscillations recorded under these quenched conditions give the phase and amplitude of the signal from a fast heat source: the generation and decay of either a 1.9 eV (650 nm) or 2.1 eV (590 nm) excited species in the solution. In order to detect the slower decay of ^{3}C-P, an unquenched sample was prepared by flushing the solution with argon to remove the oxygen so that the ^{3}C-P relaxation was characteristic of the triplet carotenoid (τ=5 μs). The PZT signal ($S_{\text{unquenched}}$) recorded after flash excitation under these conditions consists of a fast component and a slow, phase shifted component.

Quantitatively, the data in Figure 9 for an unquenched sample of C-P was fit to the convolution expression

$$S_{unquenched}(t) = a \bullet S_{quenched}(t) + b \bullet \int_{-\infty}^{t} dt' \left[\frac{1}{\tau} e^{-(t-t')} \right] S_{quenched}(t')$$

and values of a, the fraction of fast heat, b, the fraction of slow heat, and τ, the carotenoid triplet lifetime, were extracted. It is apparent from the residuals that the fit is excellent. Parameter b can be used to calculate $\Phi_t E_t$, the product of the quantum yield of carotenoid triplet (Φ_t) and the energy (E_t) of the triplet state, e.g. $b = \Phi_t E_t / (h\nu - \Phi_{fl} E_s)$ where Φ_{fl} is the fluorescence quantum yield, E_s is the energy of the lowest excited singlet state, and hν is the photon energy.

In order to demonstrate that the parameters did indeed change as a function of Φ_t and τ, experiments were carried out in which these parameters were systematically altered. The external heavy atom effect of diiodomethane at five different concentrations (including zero) was used to increase the porphyrin intersystem crossing yield (and thereby the carotenoid triplet yield) and

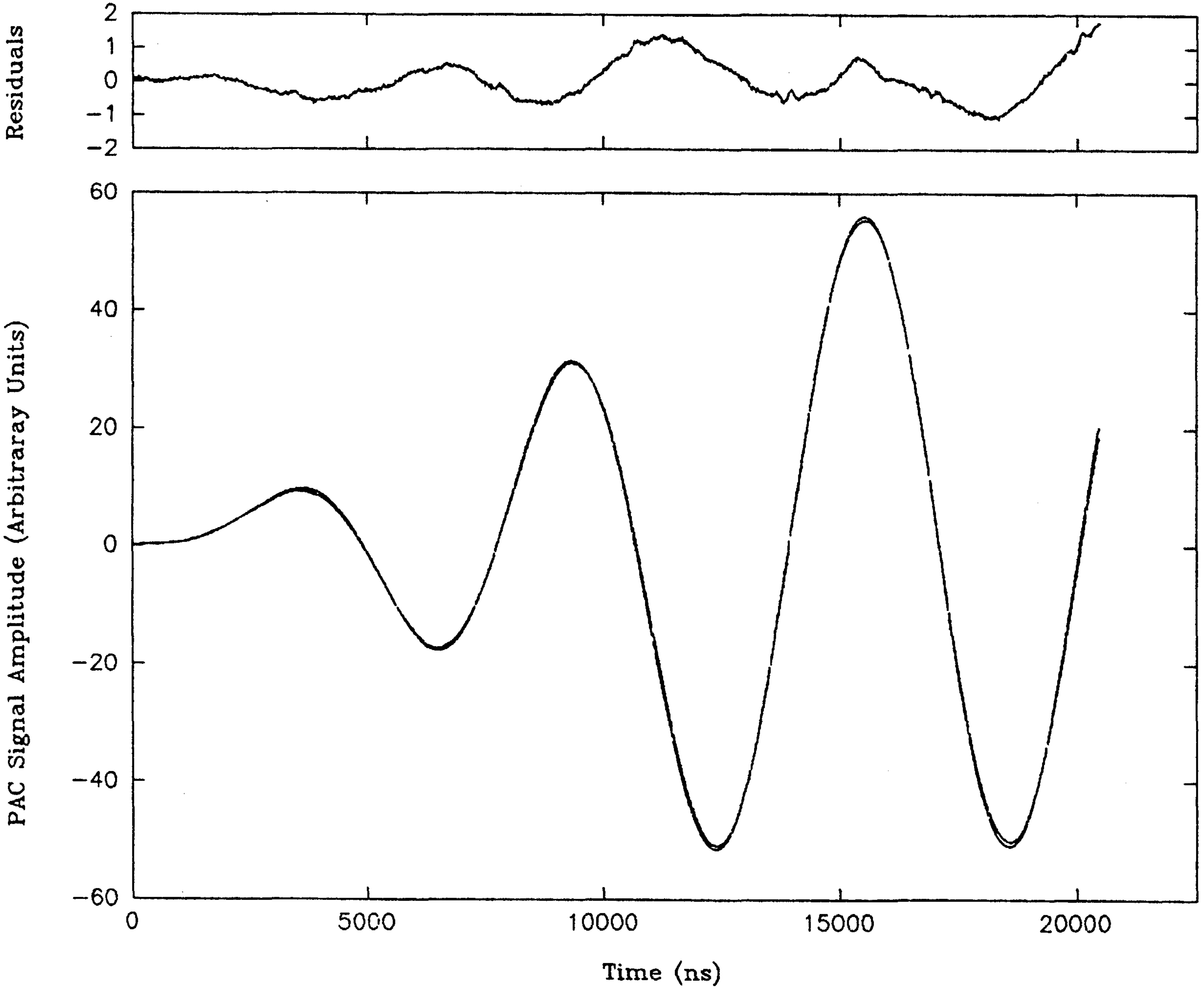

PAC Signal Amplitude and Fit VS Time Including Residuals

Figure 9

reduce the carotenoid triplet lifetime. At each diiodomethane concentration, Φ_t and τ were determined by conventional flash measurements on the same solutions used for the photoacoustic experiments. The photoacoustic signal was recorded at five different laser flash intensities for each concentration of diiodomethane. Each of the above 25 experiments was run at both 650 nm and 590 nm excitation wavelengths, for a total of 50 data sets. Since each data set involved recording the quenched and unquenched signal, there were 100 separate experiments carried out. Each experiment was then repeated so that there were actually 200 files of data generated.

At each diiodomethane concentration and excitation wavelength, the quenched and unquenched data were normalized for different laser powers and an average a, b and τ extracted. Because 10% of the excitation at 590 nm is absorbed by the carotenoid moiety and converted directly to heat, b is different for the two excitation wavelengths. This gives 10 different values of $\Phi_t E_t$. Figure 10 presents the plot of $\Phi_t E_t$ vs. Φ_t from laser flash measurements. The slope of this line gives $E_t = 0.64 \pm 0.04$ eV.

It is important to point out that τ was a variable in the analysis of the photoacoustic data. Therefore, the time dependence of the slow heat source was measured photoacoustically and could be compared with the carotenoid triplet lifetime determined from laser flash transient absorption. The agreement was always within 10%, which establishes that the species detected by the transient optical experiment and the calorimetric experiment were in fact the same; ^{3}C-P. The data shown in Figure 10 come from 100 reconvolutions of the type shown in Figure 9.

Although the measurement of E_t reported here was for a synthetic carotenoid pigment, the results should be applicable to a generic carotenoid of ca. 11 conjugated double bonds such as β-carotene. It is also noted that a triplet energy of 0.64 eV corresponds to an optical transition originating at 1937 nm, which explains the lack of reports of phosphorescence. Detectors such as indium arsenide, which are not commonly found in photochemistry laboratories, will be required to detect this emission. Because the energy gap between the ground and triplet states is rather small, the triplet potential surface must be deeply embedded in the ground state potential so that nonradiative relaxation would be expected to be fast, limiting the phosphorescence yield. In this

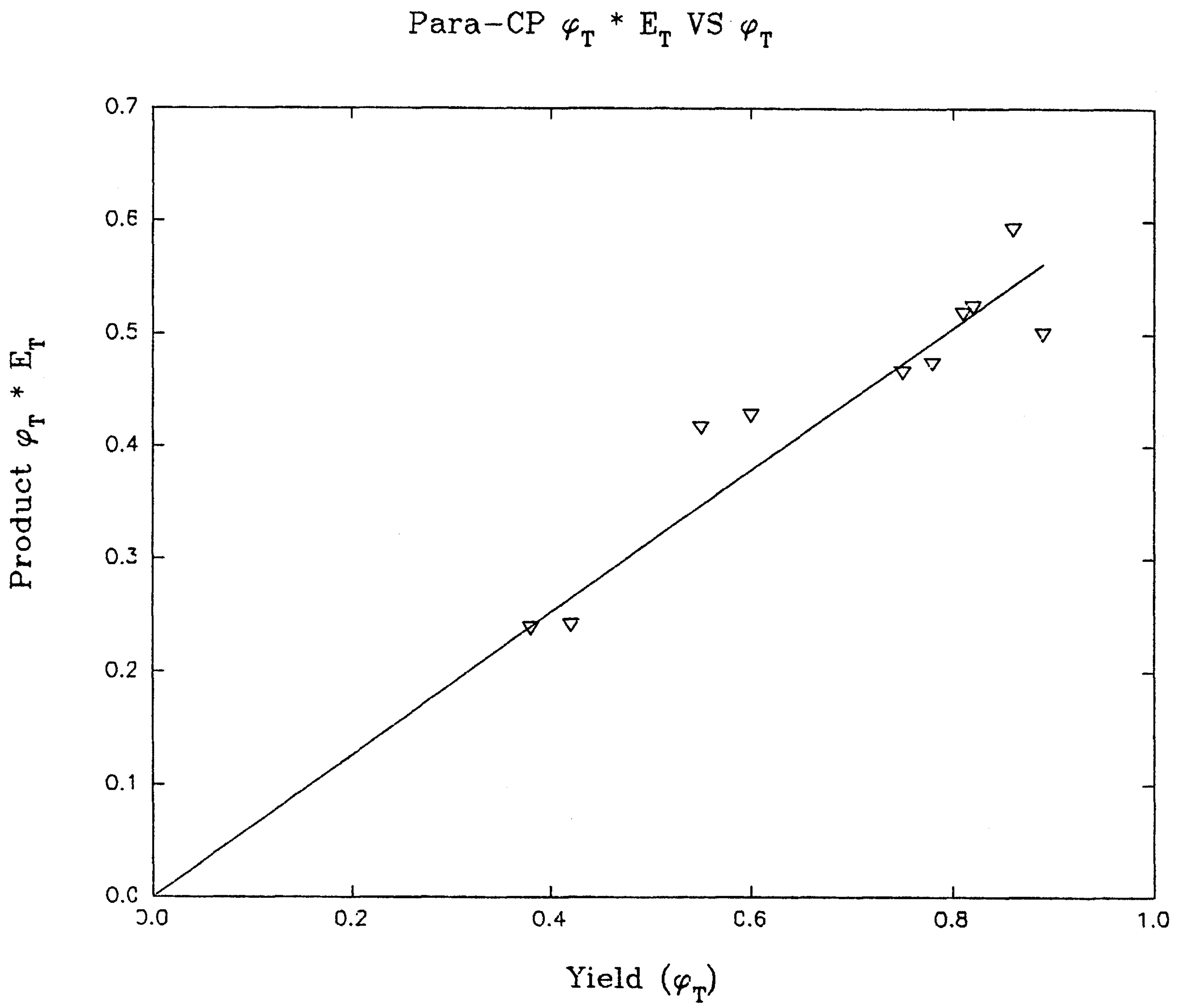
Para-CP φ_T * E_T VS φ_T
Product φ_T * E_T
0.7
0.6
0.5
0.4
0.3
0.2
0.1
0.0
0.0
0.2
0.4
0.6
0.8
1.0
Yield (φ_T)

Figure 10

connection, the short triplet lifetime of carotenoids which does not lengthen even in a frozen glassy matrix is not characteristic of the usual π, π^* triplet and is suggestive of unusually strong coupling to the ground state.

The results of these experiments are currently being written up for publication. In the future, we will be attempting to use this same photoacoustic method to determine the energies of charge-separation states in triads, tetrads and pentads.

E. Harvesting the Energy Produced by Artificial Reaction Centers: Approaches to Molecular Photovoltaics.

The long lifetimes for charge separation achieved by the pentads and other molecular photovoltaic devices mentioned above make it possible in principle to harvest the energy stored in these states by a variety of mechanisms. These include chemical reactions in solution or in multiphasic systems such as vesicles or micelles and electrical approaches including bilayer or multilayer films in electrochemical cells. Exploratory work with the electrochemical approach has led to some interesting observations which will be reported in this section. Several new approaches to this challenge are discussed in the renewal proposal.

We have begun to address the electrochemical approach to solar energy harvesting by preparing porphyrin chromophores which can be bound to conducting gold substrates through the formation of self-assembled monolayers and submonolayers. If successful, this approach could be used to bind triads, tetrads, pentads or other molecular photovoltaics to conducting substrates, and the resulting assemblies could form portions of photoelectrochemical cells for solar energy conversion.

We have investigated scanning tunneling microscopy as a technique for characterization of the bound porphyrinic materials and potentially as a method for studying their electrical and photoelectrical properties. Porphyrin species **14** and **15** have been synthesized. These molecules bear isonitrile side chains, which are known to bind to gold surfaces. We have found that immersing atomically flat (111) gold surfaces (gold evaporated onto mica) in solutions of **14** or **15** in organic solvents results in binding of the porphyrins to gold. With low exposures submonolayer coverage is achieved, while high concentrations and longer immersion times lead to self-assembly into monolayers. The resulting gold surfaces bearing porphyrins may be visualized using scanning tunneling microscopic techniques. At submonolayer coverage, individual molecules may be observed. The identity of the images is verified by the fact that we obtain a markedly larger average particle size (396Å^2) for porphyrin dyads than for monoporphyrins (121 Å^2). The STM images are strongly dependent on the sign and magnitude of the bias voltage between the STM tip and the gold surface. Thus, there is the potential for studying the electrical (and photoelectrochemical) properties of porphyrins and more complex molecular devices on conducting surfaces using this technique. Under some conditions at full monolayer coverages, the porphyrin molecules **14** or **15** are arranged in parallel ridges which maintain order over large areas of the gold surfaces. A report of this work has appeared in *Langmuir*.[13]

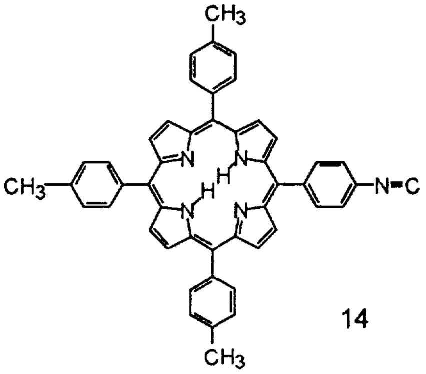

14

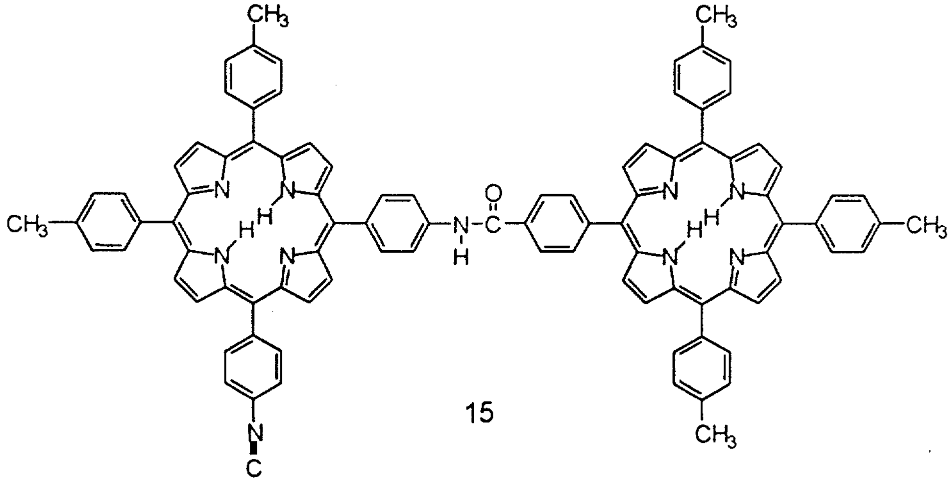

15

F. Stabilization of Charge Separation by Intramolecular Proton Transfer.

In bacterial photosynthetic reaction centers an electron is transferred from the excited state of the primary donor to quinone Q_A via ancillary tetrapyrrole(s) and then on to a second quinone Q_B. This process is then repeated. The electron transfers to Q_B involve, at some stage, its protonation to ultimately yield the hydroquinone. Although the efficiency of the forward electron transfer steps may or may not be related to protonation of this quinone in the biological system, such protonation processes are in general important in electron transfer reactions involving quinones. Thus, we have undertaken an investigation of the effect of intramolecular proton donation on electron transfer in quinone-containing synthetic reaction centers.

The purpose of our initial investigations in this area is twofold: to investigate the possibility of stabilization of energetic charge separated states via intramolecular hydrogen bonding and to devise systems in which proton transfer can be coupled to photodriven electron transfer. Triads **20, 21** and **13** are the subjects of our current experiments. Triad **20** features a *peri* hydroxyl group on the naphthoquinone moiety which can in principle serve as a proton donor to the adjacent oxygen atom. A mechanism for a possible proton transfer from the hydroxyl group which stabilizes the naphthoquinone anion radical is shown in Scheme VII.

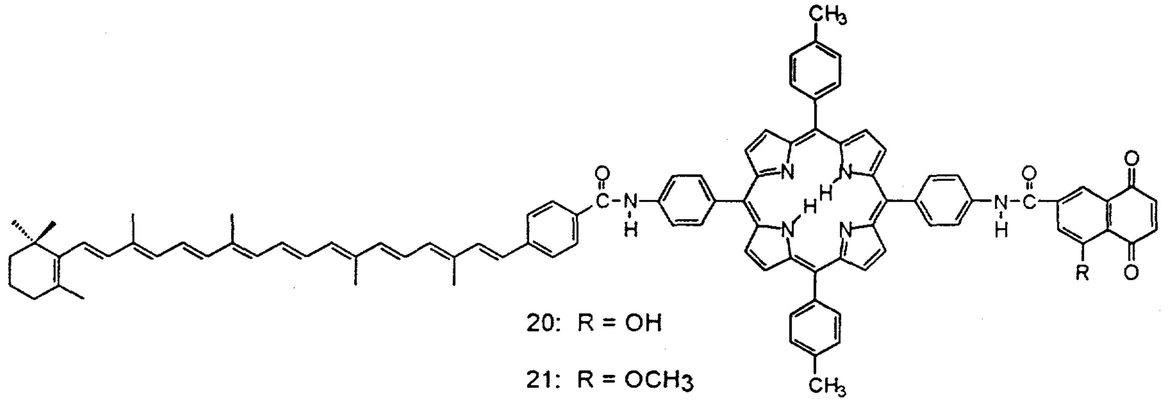

20: R = OH

21: R = OCH3

Synthesis. Triad **20** was synthesized by linking three structural units, the quinone, the porphyrin, and the carotenoid polyene moiety, via amide bonds (Scheme VIII). The protected naphthoquinone acid **22** (prepared in 5 steps from commercial 2,5-dimethoxybenzaldehyde) was

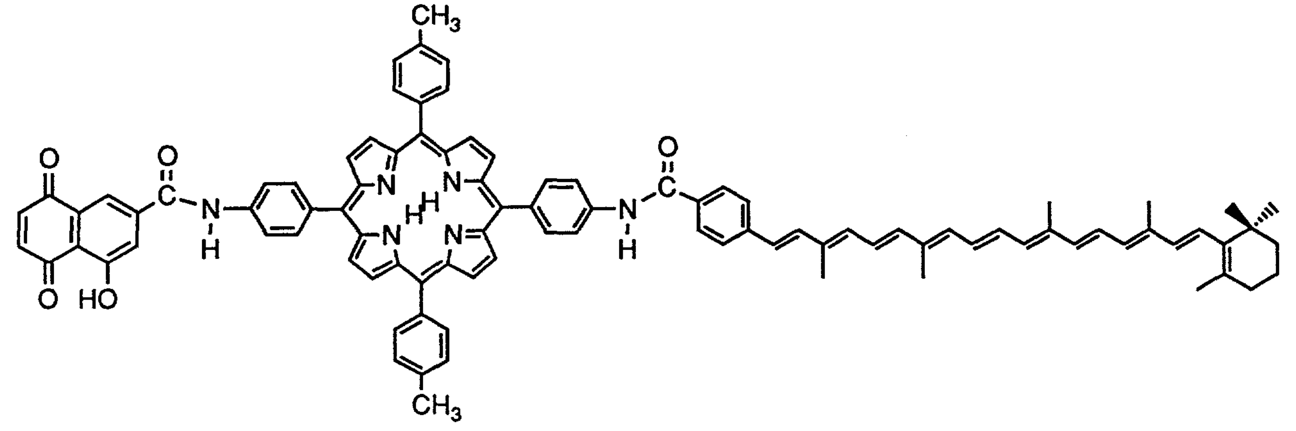

Triad **20**

Scheme VII

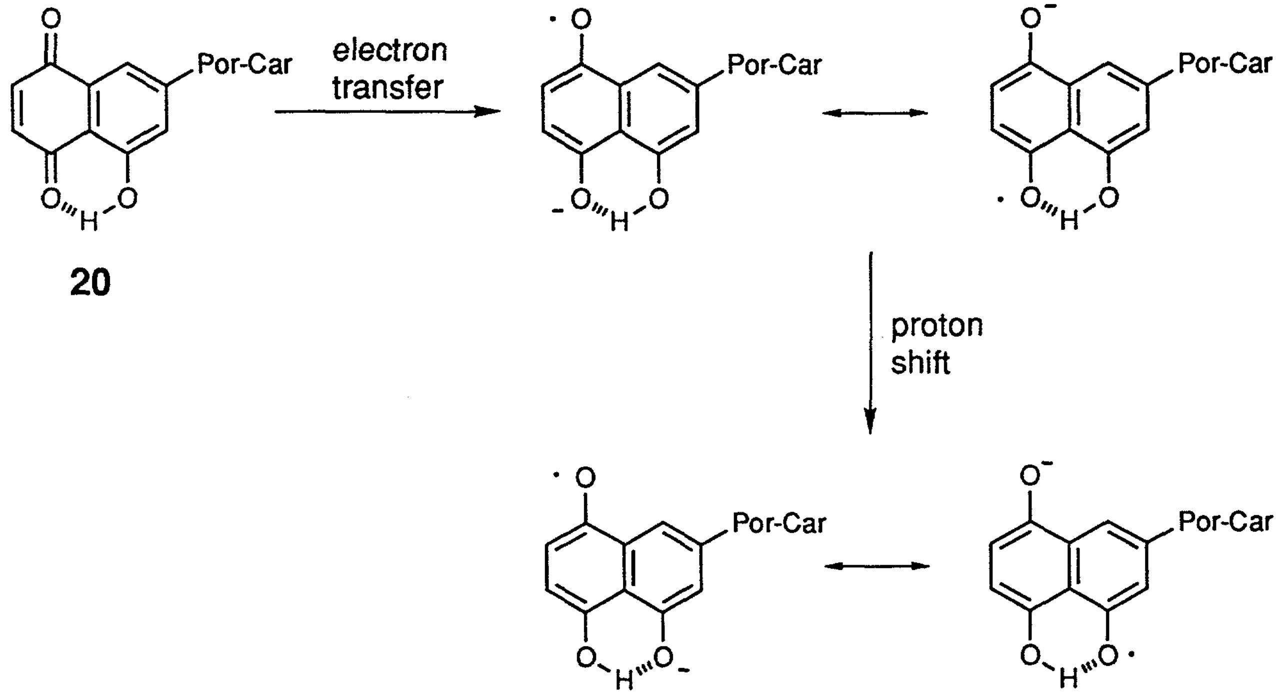

Scheme VIII

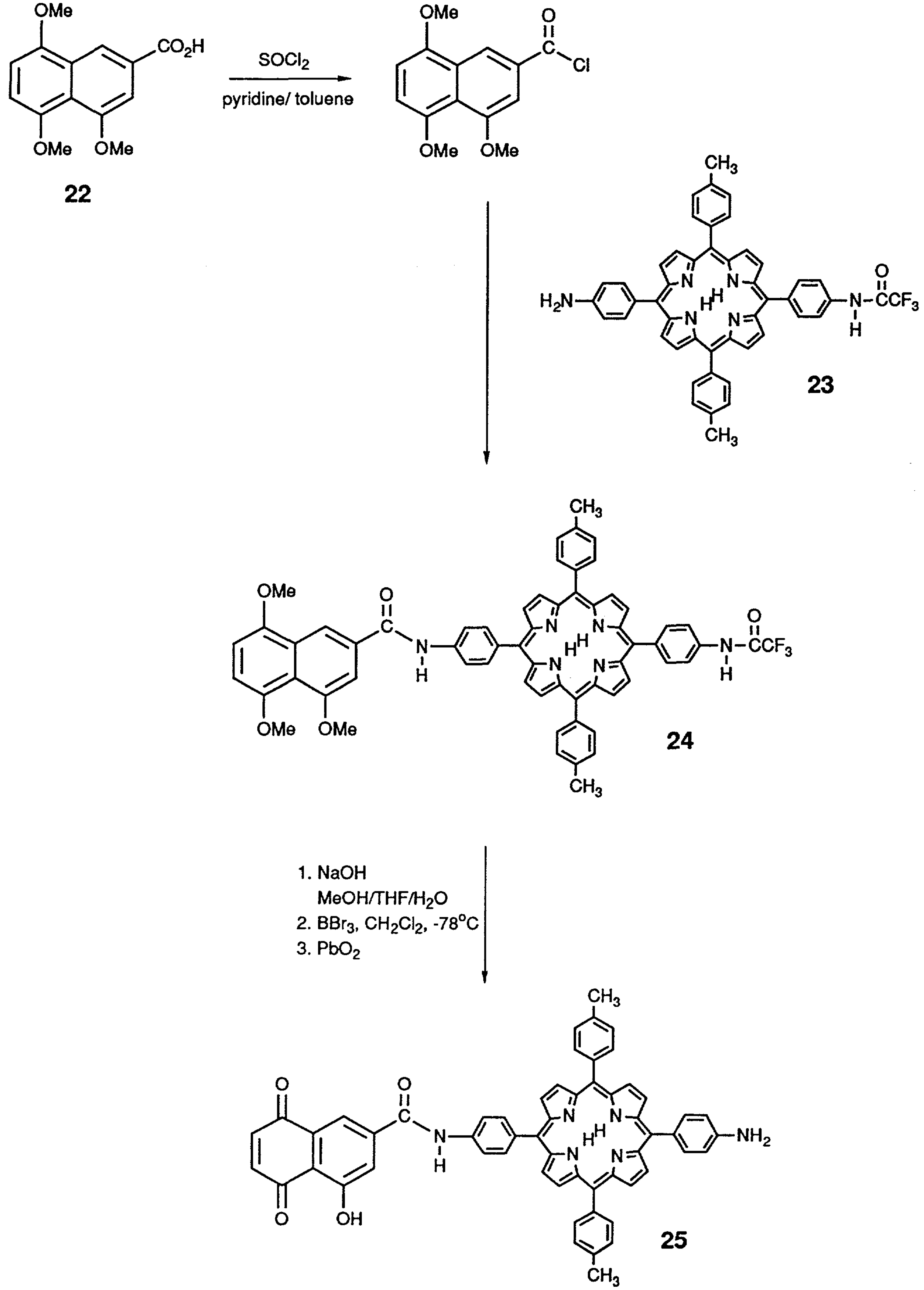
22
SOCl2
pyridine/ toluene
23
24
1. NaOH
MeOH/THF/H2O
2. BBr3, CH2Cl2, -78°C
3. PbO2
25

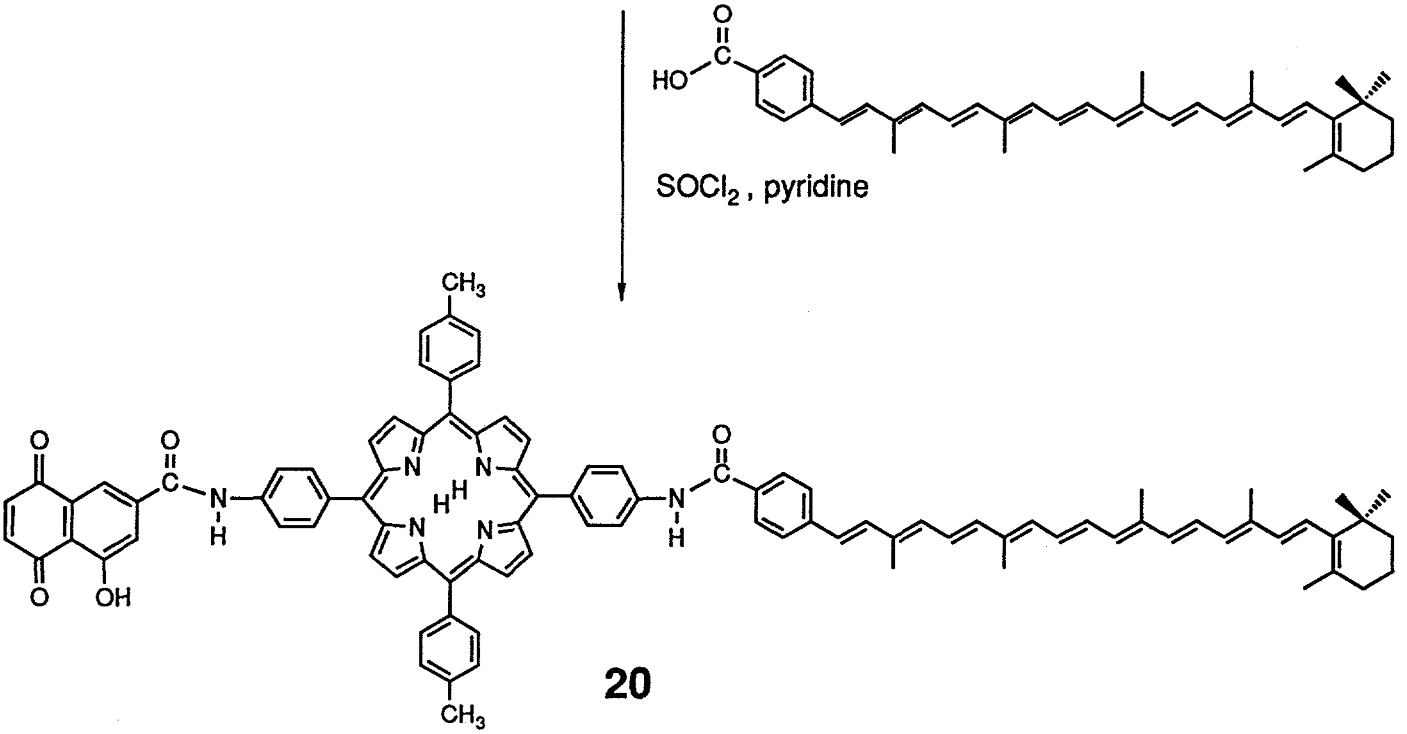

20

Table 1. Fluorescence Lifetimes and Relative Amplitudes at λ_{max}
Excitation at 590 nm

Compound	Solvent	τ_1	τ_2	χ^2
20	CH_2Cl_2	11 ps (98.1%)	87 ps (0.7%)	1.10
	$CHCl_3$	9 ps (94.1%)	40 ps (4.4%)	1.18
	$C_6H_5CN^a$	7 ps (78.7%)	42 ps (20.4%)	1.25
21	CH_2Cl_2	92 ps (96.8%)	3.4 ns (2.5%)	1.10
	$CHCl_3$	54 ps (96.7%)	3.7 ns (2.5%)	1.13
	C_6H_5CN	193 ps (96.4 %)	3.3 ns (1.8%)	1.13
13	CH_2Cl_2	67 ps (87.7%)	3.6 ns (9.0%)	1.11
	$CHCl_3$	35 ps (82.8%)	3.9 ns (5.9%)	1.12
	C_6H_5CN	113 ps (85.0%)	2.1 ns (11.9%)	1.19

[a] Excitation at 580 nm

coupled with porphyrin **23** to form **24**. The removal of the protecting groups followed by oxidation with lead dioxide gave **25**, which was then coupled to the carotenoid acid chloride to give triad **20**. Model triads **21** and **13**, which are not capable of acting as proton donors, were prepared in a related fashion.

Fluorescence and electrochemical studies. Fluorescence lifetimes of triads **20**, **21**, and **13** were determined in three solvents (dichloromethane, chloroform, and benzonitrile) at ambient temperature. Fluorescence decay curves at 7 wavelengths were obtained using the single photon timing method and analyzed using the global technique. In all cases a satisfactory fit could be obtained with one major decay component and one minor contributor (Table 1). The major component is assumed to represent the decay of the triad C-^{1}P-Q state. In all three solvents, the lifetime of triad **20** is shortest, whereas that of triad **21** is the longest. An explanation for this trend is provided by the results of electrochemical studies. Cyclic voltammetric measurements were carried out with model quinones for triads **20**, **21**, and **13**. The first reduction potentials vs. SCE were -0.403, -0.638 and -0.579 V, respectively. Thus, the longer the fluorescence lifetime, the higher the energy of the C-P$^{\bullet+}$-Q$^{\bullet-}$ state, and the lower the driving force for photoinduced electron transfer.

Nanosecond transient absorption studies. Preliminary results from transient absorption studies on the nanosecond time scale are listed in Table 2. The quantum yields and lifetimes of the final charge-separated state C$^{\bullet+}$-P-Q$^{\bullet-}$ were determined by monitoring the carotenoid radical cation absorption at 970 nm as described earlier.

Table 2. Quantum yields (Φ) and lifetimes (τ) of C$^{\bullet+}$-P-Q$^{\bullet-}$ in various solvents.

Cmpd	Φ (τ)		
	CH_2Cl_2	$CHCl_3$	C_6H_5CN
20	4% (55 ns)	4% (45 ns)	16% (70 ns)
21	3% (50 ns)	5% (29 ns)	5% (53 ns)
13	5% (57 ns)	7% (40 ns)	9% (60 ns)

Discussion. From the results of these preliminary studies, it appears that the attachment of a hydroxyl group in the *peri* position of the naphthoquinone leads to a more easily reduced electron acceptor and a concomitant increase in driving force for charge separation and decrease in driving force for charge recombination (see Scheme VI). If we assume that the charge recombination of C-$P^{\bullet +}$-$Q^{\bullet -}$ (step 2 in the Scheme) occurs in the inverted region of the Marcus relationship, then recombination in **20** would be expected to be faster than in **21** or **13.** Forward electron transfer by step 3 to yield the final $C^{\bullet +}$-P-$Q^{\bullet -}$ state should occur at essentially the same rate for all three molecules, as it does not involve porphyrin-quinone transfer. According to this reasoning, the yield of $C^{\bullet +}$-P-$Q^{\bullet -}$ would be lower in **20** than in the other two triads. However, this was not observed (Table 2). In fact, in benzonitrile, **20** has a substantially higher quantum yield than did the other two molecules. The higher yield for the final charged separated state in **20** can be explained by postulating that in this solvent, the coupled electron transfer and proton shift required in step 2 slows this step so that forward electron transfer by step 3 can compete better with it.

The accompanying proposal delineates planned investigations of this and related systems which should either verify or refute this interesting possibility.

G. Artificial Reaction Centers With Fixed Molecular Geometries.

The protein matrix which envelops the organic cofactors in natural reaction centers presumably permits very little in the way of motional reorientation of these cofactors before or after electron transfer. Reorganization of the protein matrix surrounding the cofactors in connection with electron transfer is also thought to be minimal. This is not the case in the majority of the model reaction centers prepared to date. For example, nearly all of the reported covalently-linked porphyrin quinone species have single bonds in the linkage joining the moieties, and this in turn raises the possibility that internal motions of the molecule may play some role in the various electron transfer events. One of the goals of the current grant period was to design new linkages with fixed molecular geometries. Two such molecules, porphyrin-quinone dyads **26** and **27**, have been prepared. Both feature a very rigid bicyclic bridge between the porphyrin and quinone. Continued spectroscopic investigation of these structures and their elaboration into more complex molecular devices forms an important part of the accompanying renewal proposal.

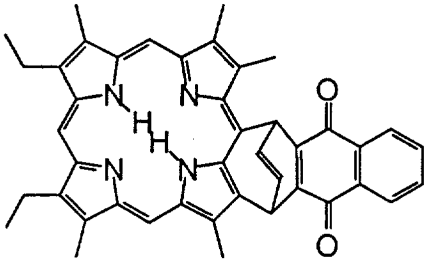

26

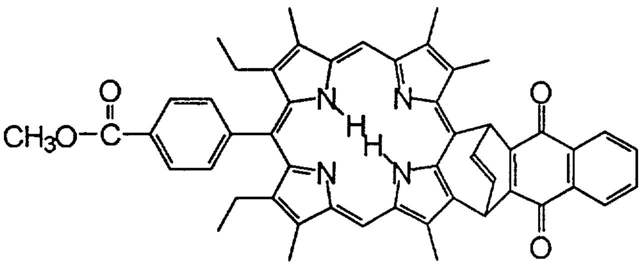

27

The synthesis of dyad **27** is outlined in Scheme IX. Dyad **26** was prepared in an analogous fashion. The introduction of the 7-membered ring on the porphyrin skeleton is a new development in porphyrin chemistry. Porphyrins such as **28** (Scheme IX) and the corresponding analog leading to **26** are designed as dienes which will take part in the Diels-Alder reaction to yield bicyclic products. Indeed, treatment of **28** with naphthoquinone at 176° C in a sealed tube evidently led to the Diels-Alder cyclization product, which was oxidized to the quinone during the reaction or subsequent workup. As discussed in the accompanying proposal, these dienes can serve as precursors to a wide variety of rigid multicomponent molecules.

The structures of **26** and **27** were assigned by mass spectrometry and extensive ^{1}H-NMR studies. Figure 11, for example, shows the proton structural relationships deduced from COSY and NOESY two-dimensional NMR experiments. Hydrogen-carbon connectivities were obtained from HMBC experiments. It has been possible from such experiments to assign all proton and most ^{13}C resonances for these molecules.

Cyclic voltammetric measurements on **26** and related model compounds at a glassy carbon electrode in benzonitrile lead to an estimate for the energy of the $P^{\bullet+}$-$Q^{\bullet-}$ state in these molecules of 1.56 eV above the ground state. The first excited singlet state of the porphyrin

Scheme IX

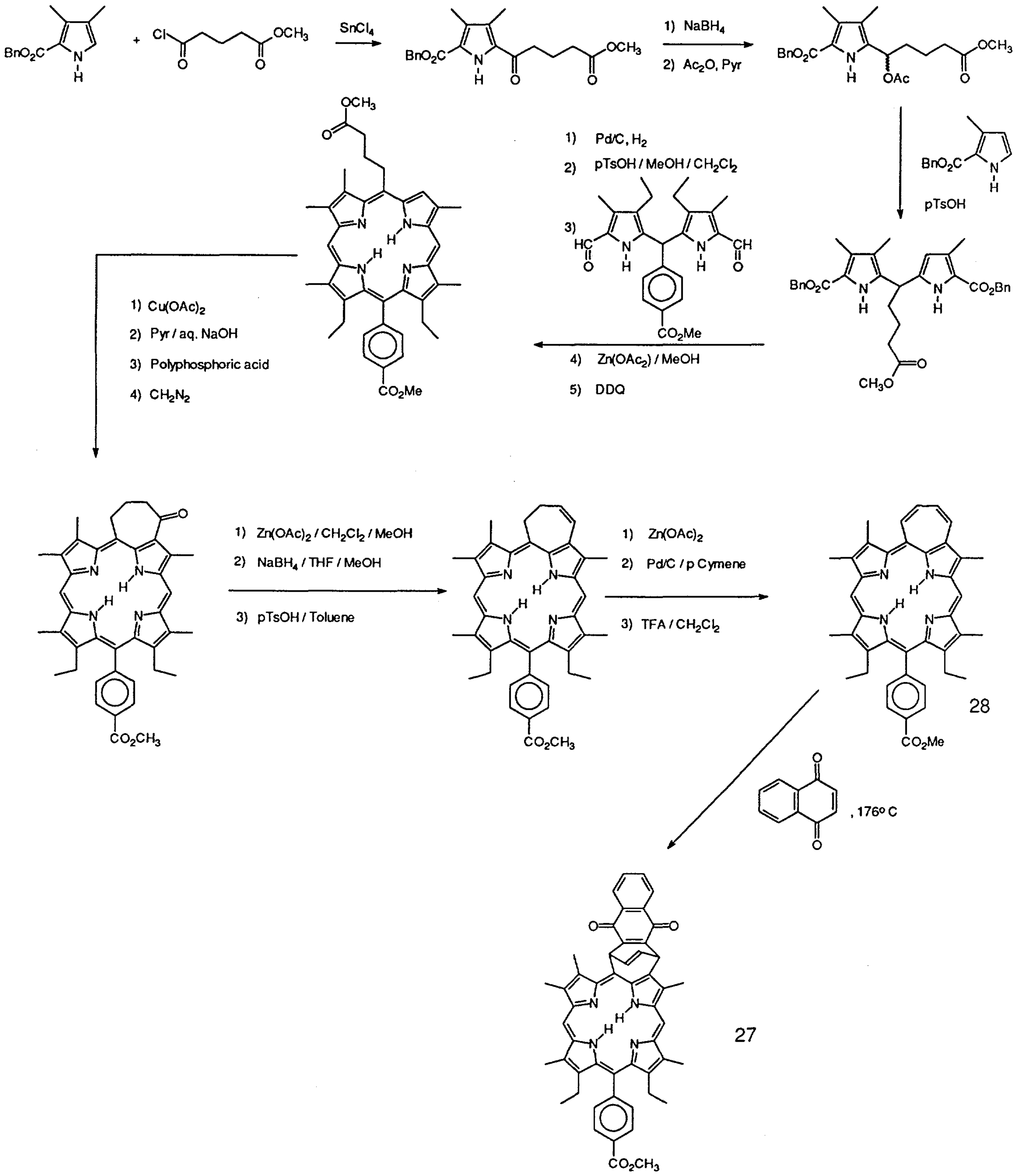
BnO_2C
+
Cl
OCH_3
$SnCl_4$
1) $NaBH_4$
2) Ac_2O, Pyr
OAc
pTsOH
CO_2Bn
CH_3O
1) Pd/C, H_2
2) pTsOH / MeOH / CH_2Cl_2
3)
HC
CH
CO_2Me
4) $Zn(OAc_2)$ / MeOH
5) DDQ
1) $Cu(OAc)_2$
2) Pyr / aq. NaOH
3) Polyphosphoric acid
4) CH_2N_2
CO_2CH_3
1) $Zn(OAc)_2$ / CH_2Cl_2 / MeOH
2) $NaBH_4$ / THF / MeOH
3) pTsOH / Toluene
1) $Zn(OAc)_2$
2) Pd/C / p Cymene
3) TFA / CH_2Cl_2
28
, 176° C
27

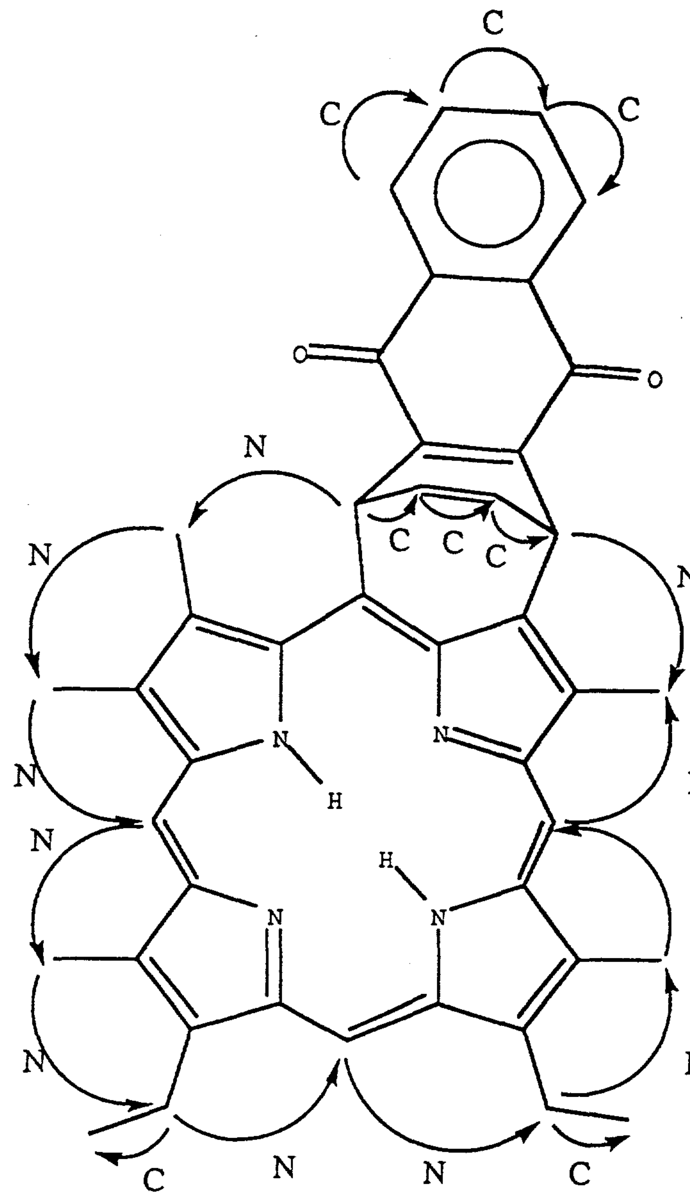

Figure 11

moiety lies at 1.93 eV. Thus, the thermodynamic driving force for photoinduced electron transfer in **26** and **27** is 0.37 eV in benzonitrile at ambient temperatures.

Preliminary time resolved absorption and fluorescence investigations of these molecules have been performed. Transient absorption experiments at 298 K in 2-methyltetrahydrofuran show that excitation of the porphyrin moiety of **27** at 590 nm with a 150-fs laser pulse produces a transient state with an absorption in the 630-640 nm region. This transient rises with a time constant of about 1 ps (Figure 12) and decays with a lifetime of 13 ps (Figure 13). Both the porphyrin first excited singlet state and the porphyrin radical cation have absorbance in this spectral region, and it is difficult to distinguish between them on spectral grounds alone. Consequently, fluorescence decay experiments were undertaken in order to determine the lifetime of the ^{1}P-Q state. A 2-methyltetrahydrofuran solution of **27** was excited at 590 nm and the fluorescence decay was measured at 713 nm, which is the maximum of the porphyrin emission. The only significant component of the decay had a lifetime of 2 ps (χ^2 = 1.12), which is shorter than the minimum time resolution of the fluorescence spectrometer. As this spectrometer readily distinguishes between fluorescence lifetimes of 2 and 13 ps, the lifetime of ^{1}P-Q in **27** must be on the order of 2 ps or less. A model porphyrin has a singlet state lifetime of 11 ns under these conditions. Thus, the ~1.0 ps rise time seen in the transient absorption experiment represents the decay of ^{1}P-Q and the concurrent rise of $P^{\bullet+}$-$Q^{\bullet-}$, whereas the 13-ps decay represents the lifetime of the $P^{\bullet+}$-$Q^{\bullet-}$ charge-separated state.

Spectroscopic investigations have also been performed at 77 K in a 2-methyltetrahydrofuran glass. The transient absorption studies showed a rise in the 630-640 nm region with a time constant of ~1 ps and a decay with a lifetime of 170 ps. These short lifetimes indicate that the porphyrin first excited singlet state is also quenched at 77 K, and thus that electron transfer is rapid even at that temperature. Low-temperature fluorescence decay studies are planned in order to determine the lifetime of ^{1}P-Q. These should establish whether the 170-ps decay represents the lifetime of charge separation, or of the porphyrin singlet state (with more rapid recombination of the ionic state).

Figure 12

RIGID PQ IN MTHF (3–4–93)
RPQCHDK.SPG: 630–640NM, 0.71PS(RISE), 13.3PS(DECAY,FIXED)

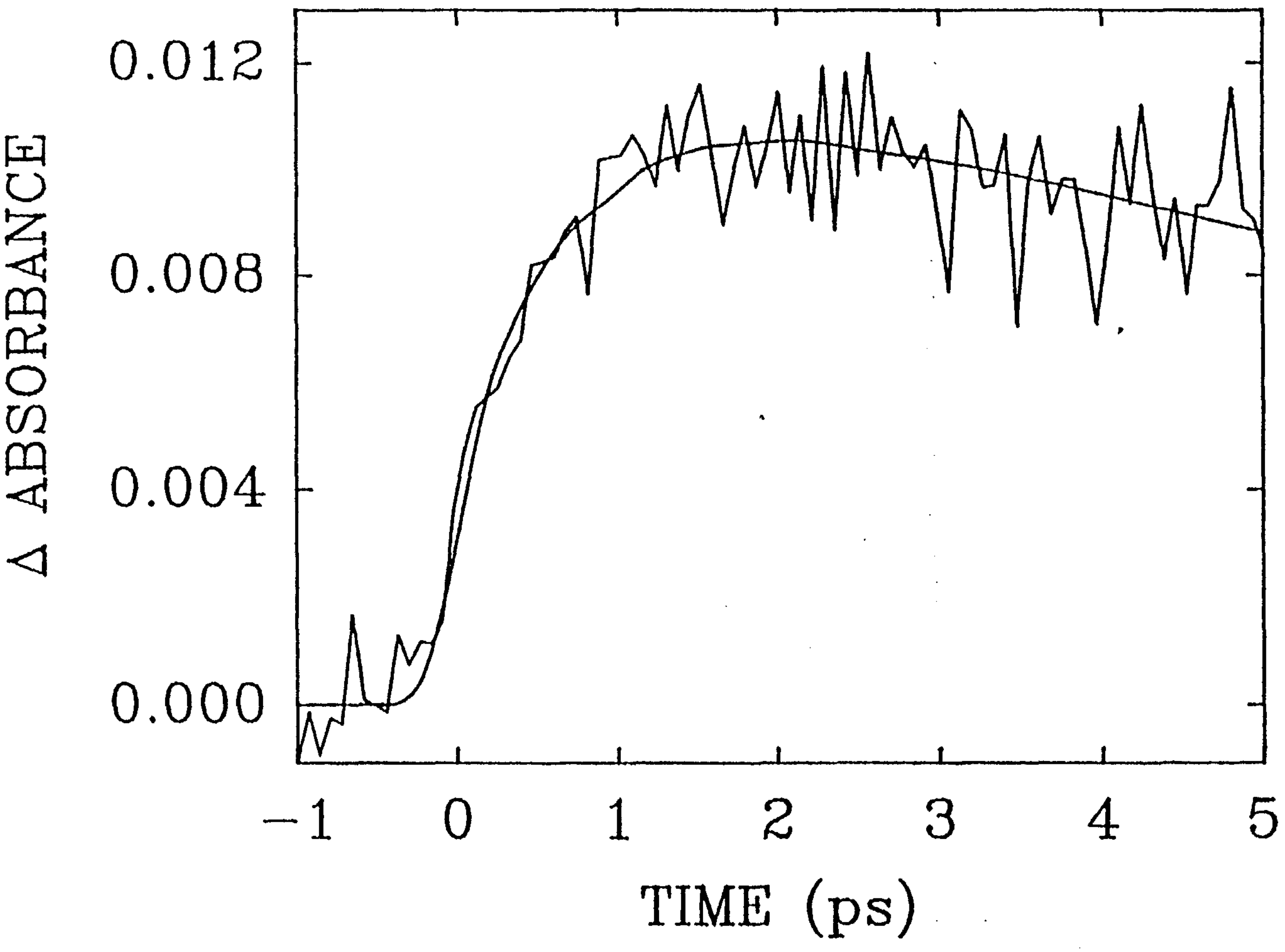

Figure 13

RPQIRDK.SPG: AVE.630−640NM, 0.63PS(RISE), 13.3PS(DECAY)
RIGID PQ IN MTHF (3−4−93)

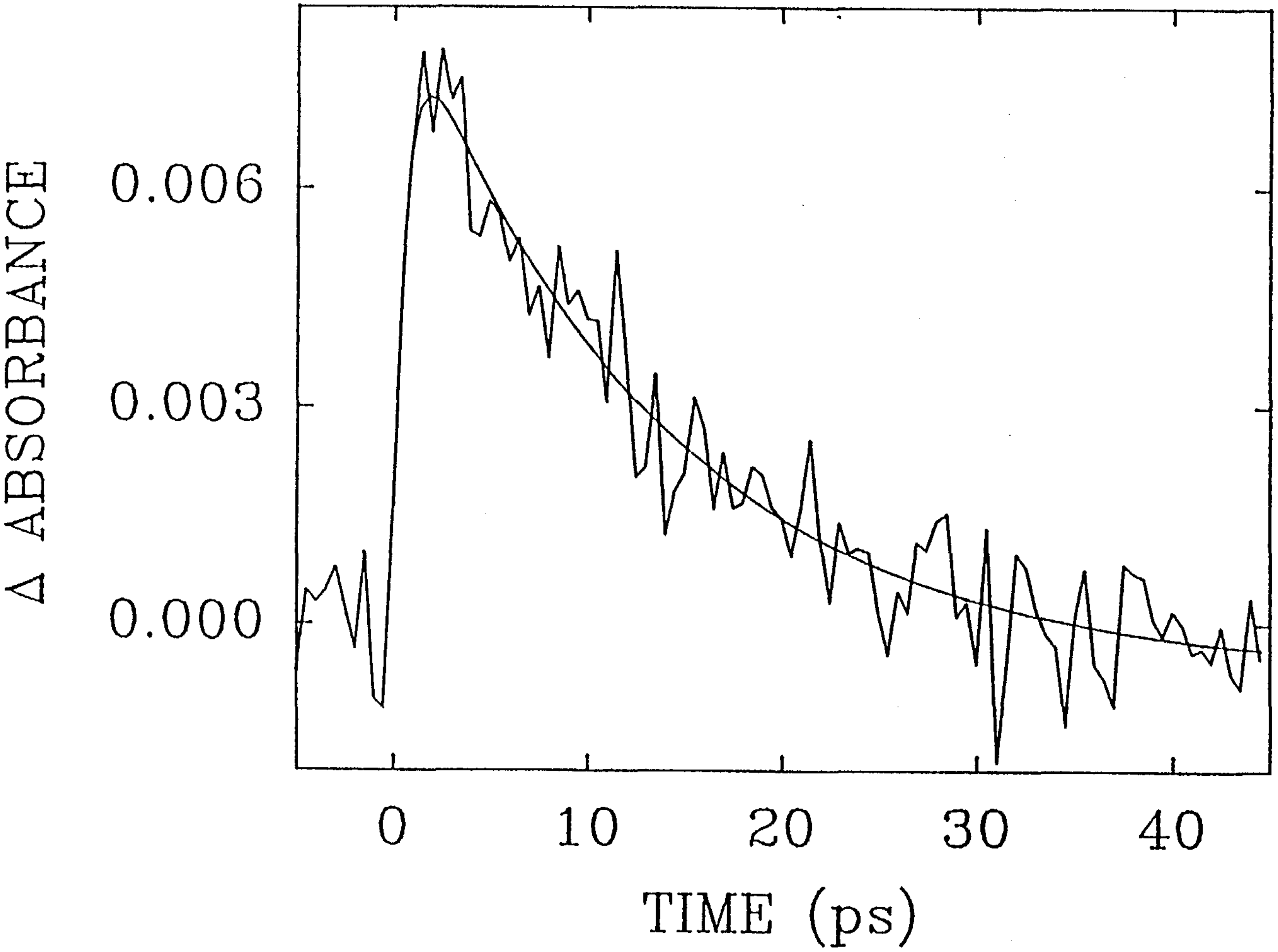

It is clear from these preliminary results that photoinduced electron transfer in **26** and **27** is extremely rapid at ambient temperatures, and also very fast in a glass at 77 K. This is very interesting, as the thermodynamic driving force for electron transfer in a polar solvent is only 0.37 eV. In many porphyrin-quinone donor-acceptor systems (such as triad **10**, for example), the thermodynamic driving force is larger in polar solvents, but electron transfer is slower, and ceases at 77 K. This is commonly attributed to a lack of stabilization of the charge-separated state by solvent in the frozen system and a consequent increase in energy of that state by ca. 0.8 eV. Clearly, an increase in the energy of $P^{\bullet+}$-$Q^{\bullet-}$ of this magnitude in **27** would make electron transfer hopelessly endergonic at 77 K. The accompanying renewal proposal outlines some planned investigations of electron transfer in these rigid systems with relatively strong electronic coupling which may shed some light on this mystery.

H. References and Notes.

1. Gust, D.; Moore, T. A.; Moore, A. L.; Macpherson, A. N.; Lopez, A.; DeGraziano, J. M.; Hung, S.-C.; Gouni, I.; Bittersmann, E.; Seely, G. R.; Gao, F.; Nieman, R. A.; Ma, X. C.; Demanche, L.; Luttrull, D. K.; Lee, S.-J.; Kerrigan, P. K. *J. Amer. Chem. Soc.* **1993**, submitted for publication.

2. Gust, D.; Moore, T. A.; Moore, A. L.; Lee, S.-J.; Bittersmann, E.; Luttrull, D. K.; Rehms, A. A.; DeGraziano, J. M.; Ma, X. C.; Gao, F.; Belford, R. E.; Trier, T. T. *Science* **1990**, *248*, 199-201.

3. Hermant, R. M.; Liddell, P. A.; Lin, S.; Alden, R. G.; Kang, H. K.; Moore, A. L.; Moore, T. A.; Gust, D. *J. Am. Chem. Soc.* **1993**, *115*, 2080-2081.

4. Lee, S.-J.; DeGraziano, J. M.; Macpherson, A. N.; Shin, E.-J.; Seely, G. R.; Kerrigan, P. K.; Moore, A. L.; Moore, T. A.; Gust, D. *Chem. Phys.* **1993**, submitted for publication.

5. Gust, D.; Moore, T. A.; Moore, A. L.; Barrett, D.; Harding, L. O.; Makings, L. R.; Liddell, P. A.; De Schryver, F. C.; Van der Auweraer, M.; Bensasson, R. V.; Rougée, M. *J. Am. Chem. Soc.* **1988**, *110*, 321-323.

6. Gust, D.; Moore, T. A.; Moore, A. L.; Seely, G.; Liddell, P.; Barrett, D.; Harding, L. O.; Ma, X. C.; Lee, S.-J.; Gao, F. *Tetrahedron* **1989**, *45*, 4867-4891.

7. Moore, T. A.; Gust, D.; Mathis, P.; Mialocq, J.-C.; Chachaty, C.; Bensasson, R. V.; Land, E. J.; Doizi, D.; Liddell, P. A.; Lehman, W. R.; Nemeth, G. A.; Moore, A. L. *Nature (London)* **1984**, *307*, 630-632.

8. Gust, D.; Moore, T. A.; Liddell, P. A.; Nemeth, G. A.; Makings, L. R.; Moore, A. L.; Barrett, D.; Pessiki, P. J.; Bensasson, R. V.; Rougee, M.; Chachaty, C.; De Schryver, F. C.; Van der Auweraer, M.; Holzwarth, A. R.; Connolly, J. S. *J. Am. Chem. Soc.* **1987**, *109*, 846-856.

9. Gust, D.; Moore, T. A.; Makings, L. R.; Liddell, P. A.; Nemeth, G. A.; Moore, A. L. *J. Am. Chem. Soc.* **1986**, *108*, 8028-8031.

10. Hung, S.-C.; Lin, S.; Macpherson, A. N.; DeGraziano, J. M.; Kerrigan, P. K.; Liddell, P. A.; Moore, A. L.; Moore, T. A.; Gust, D. *J. Photochem. Photobiol.* **1993**, submitted for publication.

11. Hasharoni, K.; Levanon, H.; Tang, J.; Bowman, M. K.; Norris, J. R.; Gust, D.; Moore, T. A.; Moore, A. L. *J. Am. Chem. Soc.* **1990**, *112*, 6477-6481.

12. Hasharoni, K.; Levanon, H.; Bowman, M. K.; Norris, J. R.; Gust, D.; Moore, T. A.; Moore, A. L. *Applied Magnetic Resonance* **1990**, *1*, 357-368.

13. Luttrull, D. K.; Graham John,; DeRose, J. A.; Gust, D. M. T. A.; Lindsay, S. M. *Langmuir* **1992**, *8*, 765-768.

Publications and Meeting Presentations Resulting From This Project (1990 - 1993)

Publications:

1. "Efficient Multistep Photoinitiated Electron Transfer in a Molecular Pentad," D. Gust, T. A. Moore, A. L. Moore, S.-J. Lee, E. Bittersmann, D. K. Luttrull, A. A. Rehms, J. M. De Graziano, X. C. Ma, F. Gao, R. E. Belford and T. T. Trier, *Science*, **248**, 199-201 (1990).

2. "Association of Chlorophyll with Inverted Micelles of Dodecylpyridinium Iodide in Toluene," G. R. Seely, X. C. Ma, R. A. Nieman and D. Gust, *J. Phys. Chem.*, **94**, 1581-1586 (1990).

3. "Singlet Photochemistry in Model Photosynthesis: Identification of Charge Separated Intermediates by Fourier Transform and CW EPR Spectroscopies," K. Hasharoni, H. Levanon, J. Tang, M. K. Bowman, J. R. Norris, D. Gust, T. A. Moore and A. L. Moore, *J. Am. Chem. Soc.*, **112**, 6477-6481 (1990).

4. "Analysis of Time-Resolved CW-EPR Spectra of Short-Lived Radicals at Different Times After Laser Excitation," K. Hasharoni, H. Levanon, M. K. Bowman, J. R. Norris, D. Gust, T. A. Moore and A. L. Moore, *Applied Magn. Reson.*, **1**, 357-368 (1990).

5 "Multistep Photoinitiated Charge Separation in a Molecular Pentad," T. A. Moore, D. Gust, A. L. Moore, S.-J. Lee, E. Bittersmann, D. K. Luttrull, J. M. DeGraziano, X. C. Ma and F. Gao, *Proceedings of the Twelfth Annual International Conference of the IEEE/EMBS*, **12**, 1737-1738 (1990).

6 "Photosynthetic Model Systems," D. Gust and T. A. Moore, *Topics in Current Chemistry*, **159**, 103-151 (1991).

7 "Mimicking Photosynthetic Electron and Energy Transfer," D. Gust and T. A. Moore, *Advances in Photochemistry*, **16**, 1-65 (1991).

8 "Mimicking Photosynthetic Electron Transfer," D. Gust, T. A. Moore and A. L. Moore, In: *Materials Synthesis Based on Biological Processes*, M. Alper, P. Clavert, R. Frankel, P. Rieke and D. Tirrell, eds. (Pittsburgh: Materials Research Society), 141-152 (1991).

9. Imaging Porphyrin-Based Molecules on a Gold Substrate in Ambient Conditions," D. K. Luttrull, J. Graham, J. A. DeRose, D. Gust, T. A. Moore and S. M. Lindsay, *Langmuir* , **8**, 765-768 (1992).

10. Synthesis of Carotenoporphyrin Models for Photosynthetic Energy and Electron Transfer," D. Gust, T. A. Moore, A. L. Moore and P. A. Liddell, *Methods in Enzymology*, **213**, 87-100, (1992).

11. Multistep Electron and Energy Transfer in Artificial Photosynthesis," D. Gust and T. A. Moore, In: *The Photosynthetic Reaction Center, Volume II*, J. Deisenhofer and J. R. Norris, eds. (New York: Academic Press), 419 - 464 (1993).

12. The Optimization of Photochemical Energy Conversion: Synthetic Supramolecular Devices vis à vis Photosynthesis," T. A. Moore, D. Gust and A. L. Moore, In *Supramolecular Chemistry,* V. Balzani and L. De Cola, eds. (Amsterdam, Kluwer), 295-311 (1992).

13 "Mimicking Photosynthetic Energy and Electron Transfer," D. Gust, T. A. Moore and A. L. Moore, *Proceedings of the Ninth International Conference on Photochemical Conversion and Storage of Solar Energy,* in press.

14. Synthesis of New Carotenoids for Photosynthetic Model Systems," B.-L. Liu, D. Gust, T. A. Moore and A. L. Moore, In *Research in Photosynthesis, Vol. II,* N. Murata, ed. (Amsterdam, Kluwer), 801 - 804 (1992).

15. "Molecular Mimicry of Photosynthetic Energy and Electron Transfer," D. Gust, T. A. Moore and A. L. Moore, *Accounts of Chemical Research*, in press.

16. "Photosynthesis Mimics as Molecular Electronics Devices," D. Gust, T. A. Moore and A. L. Moore, *IEEE Engineering in Medicine and Biology Magazine*, in press.

17. "The Photochemistry of Carotenoids. Some Photosynthetic and Photomedical Aspects," D. Gust, T. A. Moore and A. L. Moore, *Ann. New York Acad. Sci.*, in press.

18. "Photoinitiated Charge Separation in a Carotenoid-Porphyrin-Diquinone Tetrad: Enhancement of Quantum Yields via Control of Electronic Coupling," S.-J. Lee, J. M. DeGraziano, A. N. Macpherson, E.-J. Shin, G. R. Seely, P. K. Kerrigan, A. L. Moore, T. A. Moore and D. Gust, *Chem. Phys.,* submitted for publication.

19. "Kinetics of Multistep Photoinitiated Electron Transfer Reactions in a Molecular Triad," S.-C. Hung, S. Lin, A. N. Macpherson, J. M. Degraziano, P. K. Kerrigan, P. A. Liddell, A. L. Moore, T. A. Moore and D. Gust, *J. Photochem. Photobiol.,* submitted for publication.

20. "Photoinitiated Electron and Energy Transfer in Molecular Pentads," D. Gust, T. A. Moore, A. L. Moore, A. N. Macpherson, A. Lopez, J. M. DeGraziano, I. Gouni, E. Bittersmann, G. R. Seely, F. Gao, R. A. Nieman, X. C. Ma, L. Demanche, D. K. Luttrull, S.-J. Lee and P. K. Kerrigan, *J. Am. Chem. Soc.*, submitted for publication.

Meeting Presentations.

1. "Multicomponent Molecular Devices Which Mimic Photosynthetic Electron Transfer," D. Gust, U. K. Molecular Electronics Workshop, Durham, UK, July, 1990.

2. “Mimicry of Photosynthetic, Electron Transfer by a Synthetic Molecular Pentad,” D. Gust, T. A. Moore and A. L. Moore, Electron Donor-Acceptor Gordon Conference, Newport, RI, August, 1990.

3. “Mimicking Photosynthetic Electron Transfer,” D. Gust, T. A. Moore and A. L. Moore, Abstracts of the 1990 Fall Meeting of the Materials Research Society, 653 (1990).

4. “Multistep Photoinitiated Electron Transfer in Molecular Pentads and Tetrads,” D. Gust, T. A. Moore, A. L. Moore, S.-J. Lee, E. Bittersmann, D. K. Luttrull, J. M. DeGraziano, X. C. Ma and F. Gao, 14th DOE Solar Photochemistry Research Conference, Lake Harmony, PA, June, 1990.

5. “Multistep Photoinitiated Electron Transfer in Molecular Pentads, Tetrads and Triads,” D. Gust, T. A. Moore, A. L. Moore, S.-J. Lee, E. Bittersmann, D. K. Luttrull, J. M. DeGraziano, X. C. Ma and F. Gao, Eighth International Conference on Photochemical Conversion and Storage of Solar Energy, Palermo, Italy, July, 1990.

6. “Photoacoustic Detection of the Relaxation of Porphyrin, Carotenoid and Singlet Oxygen Excited Species,” T. A. Moore, D. Gust and A. L. Moore, XIIIth IUPAC Symposium on Photochemistry, Coventry, England, July, 1990.

7. “Mimicry of Photosynthetic Electron and Energy Transfer by a Synthetic Molecular Pentad,” D. Gust, T. A. Moore, A. L. Moore, S.-J. Lee, E. Bittersmann, D. K. Luttrull, J. M. DeGraziano, X. C. Ma and F. Gao, XIIIth IUPAC Symposium on Photochemistry, Coventry, England, July, 1990.

8. “Mimicry of Photosynthetic Electron Transfer by a Synthetic Molecular Pentad,” D. Gust, T. A. Moore and A. L. Moore, XIX Latin-American Congress of Chemistry, Buenos Aires, Argentina, November, 1990, Abs. OR30.

9. “Multistep Electron Transfer Strategies for Artificial Photosynthesis,” D. Gust, International Conference on Energy Conversion Science: Primary Processes of Energy Conversion in Molecular and Biological Systems, Kanagawa Science Park, Japan, February, 1991.

10. “Photoinitiated Electron Transfer in Synthetic Tetrads and Pentads,” D. Gust, T. A. Moore and A. L. Moore, Fifteenth DOE Solar Photochemistry Research Conference, Snowmass Village, Colorado, June, 1991.

11. “Multistep Electron Transfer Strategies for Artificial Photosynthesis,” D. Gust, Symposium on Electron Transfer Processes in Chemistry and Biology, Centre for Photomolecular Sciences, Imperial College, London, June, 1991.

12. “Synthetic Models for Reaction Centers,” D. Gust, Gordon Research Conference on Photosynthesis: Biophysical Aspects, July, 1991.

13. “Multicomponent Molecular Systems Which Mimic Photosynthetic Electron and Energy Transfer,” D. Gust, T. A. Moore and A. L. Moore, The 10-Year Anniversary Symposium of the

Japan-US Cooperative Photoconversion and Photosynthesis Research Program, Okazaki, Japan, December, 1991.

14. "Molecular Pentads - Synthesis and Electron Transfer Studies," A. Lopez, T. A. Moore, A. L. Moore, D. Gust, I. Gonni, J. DeGraziano, D. Luttrull and P. Kerrigan, Western Regional Photosynthesis Conference, Tempe, Arizona, January, 1991.

15. "Photochemistry of Porphyrin Monolayer Films," D. Luttrull, D. Gust, T. A. Moore, J. Graham and S. M. Lindsay, Western Regional Photosynthesis Conference, Tempe, Arizona, January, 1991.

16. "Photosynthesis by Organic Photochemists," T. A. Moore, A. L. Moore and D. Gust, 3er. Encuentro Latinoamericano de Fotoquimica y Fotobiologia, Mar del Plata, Argentina, October, 1991.

17. "The Optimization of Photochemical Energy Conversion: Synthetic Supramolecular Devices vis à vis Photosynthesis," T. A. Moore, D. Gust and A. L. Moore, II NATO Science Forum on Supramolecular Chemistry, Taromina, Sicily (Italy), December 15-18, 1991.

18. "Mimicry of Photosynthetic Energy and Electron Transfer," D. Gust, T. A. Moore and A. L. Moore, Fourth Annual Conference of the Inter-American Photochemical Society, Clearwater Beach, FL, January, 1992.

19. "Mimicking Photosynthetic Energy and Electron Transfer," D. Gust, T. A. Moore and A. L. Moore, Ninth International Conference on Photochemical Conversion and Storage of Solar Energy, Beijing, China, August, 1992.

20. "Resonance Raman Studies of Caroteno-Tetratolylporphyrin Dyads," M. H. Wall, A. L. Moore, T. A. Moore, D. Gust, P. A. Liddell and M. R. Ondrias, 203rd ACS National Meeting, San Francisco, CA, April, 1992.

21. "Electron Photoconduction by Carotenoids," A. L. Moore, D. Gust, T. A. Moore, L. Sereno, J. J. Silber, P. A. Liddell, P. Seta and E. Bienvenue, Twentieth Annual Meeting of the American Society for Photobiology, Marco Island, FL, June, 1992 (*Photochem. Photobiol.* 55, 101S (1992)).

22. "Electronic Effects on Photoinitiated Electron Transfer in Multichromophoric Systems," D. Gust, T. A. Moore, A. L. Moore, S.-J. Lee, J. M. DeGraziano, A. Lopez, I. F. Gouni and P. K. Kerrigan, Sixteenth DOE Solar Photochemistry Research Conference, Lake Geneva, WI, June, 1992.

23. "Synthesis of New Carotenoids for Photosynthetic Model Systems," B.-L. Liu, D. Gust, T. A. Moore and A. L. Moore, Ninth International Congress on Photosynthesis, Nagoya, Japan, September, 1992 (*Photosynthesis Research,* **34**, 165 (1992).

24. "Synthesis and Photoinitiated Electron Transfer in Artificial Photosynthetic Molecules," S.-J. Lee, D. Gust, T. A. Moore, A. L. Moore, E. Bittersmann, D. K. Luttrull, J. M. DeGraziano,

X. C. Ma and F. Gao, International Symposium on Photochemistry, Photobiology and Photomedicine, Taejon, Korea, September, 1992.

25. “Model Systems for Photosynthesis,” D. Gust, Western Regional Photosynthesis Conference, Asilomar, CA, January, 1993.

26. “Photochemical Reactions of Carotenoids,” D. Gust, T. A. Moore and A. L. Moore, Carotenoids in Human Health, sponsored by the New York Academy of Sciences, San Diego, CA, February, 1993.

27. "Molecular Approaches to Artificial Photosynthesis," D. Gust, T. A. Moore and A. L. Moore, 205th National Meeting of the American Chemical Society, Denver, CO, March, 1993.

28. “Photoconducting Properties of Carotenes in Monolayers,” I. Gouni, D. Gust, T. A. Moore and A. L. Moore, Western Regional Photosynthesis Conference, Asilomar, CA, January, 1993.

29. “Electron Transfer to Hydrogen Bonded Quinone Systems,” S. C. Hung, A. Moore, T. Moore, D. Gust, P. Kerrigan, Western Regional Photosynthesis Conference, Asilomar, CA, January, 1993.

30. "Synthesis and Photoinitiated Electron Transfer of a Molecular Pentad," S.-J. Lee, E.-J. Shin, J. M. DeGraziano, P. K. Kerrigan, A. Macpherson, T. A. Moore, A. L. Moore and D. Gust, 205th National Meeting of the American Chemical Society Denver, CO, March, 1993.